Check for updates

Received: 21 December 2020 | Revised: 30 March 2021 | Accepted: 6 April 2021

DOI: 10.1002/wcms.1537

ADVANCED REVIEW

WIREs COMPUTATIONAL MOLECULAR SCIENCE WILEY

Investigations of water/oxide interfaces by molecular dynamics simulations

Ruiyu Wang[1,2] | **Michael L. Klein**[1,2,3] | **Vincenzo Carnevale**[3,4] | **Eric Borguet**[1,2]

[1]Department of Chemistry, Temple University, Philadelphia, Pennsylvania, USA

[2]Center for Complex Materials from First Principles (CCM), Temple University, Philadelphia, Pennsylvania, USA

[3]Institute for Computational Molecular Science, Temple University, Philadelphia, Pennsylvania, USA

[4]Department of Biology, Temple University, Philadelphia, Pennsylvania, USA

Correspondence
Eric Borguet, Department of Chemistry, Temple University, Philadelphia, Pennsylvania 19122, USA.
Email: eborguet@temple.edu

Vincenzo Carnevale, Institute for Computational Molecular Science, Temple University, Philadelphia, PA 19122.
Email: vincenzo.carnevale@temple.edu

Funding information
Basic Energy Sciences, Grant/Award Number: #DE-SC0012575; National Institutes of Health, Grant/Award Numbers: R01GM093290, R01GM131048, S10OD020095; National Science Foundation, Grant/Award Numbers: IOS-1934848, MRI-1828421; Temple University

Edited by: Peter Schreiner, Associate Editor

Abstract

Water/oxide interfaces are ubiquitous on earth and show significant influence on many chemical processes. For example, understanding water and solute adsorption as well as catalytic water splitting can help build better fuel cells and solar cells to overcome our looming energy crisis; the interaction between biomolecules and water/oxide interfaces is one hypothesis to explain the origin of life. However, knowledge in this area is still limited due to the difficulty of studying water/solid interfaces. As a result, research using increasingly sophisticated experimental techniques and computational simulations has been carried out in recent years. Although it is difficult for experimental techniques to provide detailed microscopic structural information, molecular dynamics (MD) simulations have satisfactory performance. In this review, we discuss classical and ab initio MD simulations of water/oxide interfaces. Generally, we are interested in the following questions: How do solid surfaces perturb interfacial water structure? How do interfacial water molecules and adsorbed solutes affect solid surfaces and how do interfacial environments affect solvent and solute behavior? Finally, we discuss progress in the application of neural network potential based MD simulations, which offer a promising future because this approach has already enabled ab initio level accuracy for very large systems and long trajectories.

This article is categorized under:

Theoretical and Physical Chemistry > Spectroscopy
Molecular and Statistical Mechanics > Molecular Interactions
Structure and Mechanism > Molecular Structures

KEYWORDS

ion adsorption, molecular dynamics simulation, pKa, sum frequency generation, water/oxide interface

1 | INTRODUCTION

As one of the most ubiquitous substances on earth, water plays important roles in innumerable chemical processes. One particular system, the water/solid interface, has close relationships to geochemistry, electrochemistry, environment chemistry, and catalysis, and this attracts significant research interest.[1–4] For example, amino acid condensation, an important step of the origin of life, are more favored at mineral surfaces than in bulk water[5,6]; water/platinum

 © 2021 Wiley Periodicals LLC.

interfaces are widely used as electrodes for electrochemistry applications[7]; hydrogen fuel, believed to be one of the solutions to energy crisis, can be produced via water oxidation or hydrogen evolution reactions catalyzed by manganese oxide or MoS_2,[8,9] and investigating these water/material interfaces can reveal the catalytic mechanisms and lead to the optimization of material design. In recent years, thousands of research articles have been published, but the answer to many fundamental questions, such as how far away from the solid surface is the solvent affected, how adsorbed solutes perturb interfacial water and the solid surfaces, and how chemical reactions at interfaces are different from those in the bulk, are still unknown or controversial.

A number of electrical double layer theory (EDL) models have been developed for describing the structure of charged solid/water interfaces.[10] In these models, the solid surface is treated as a homogenous infinite flat charged panel without any microscopic description of the chemical structure, and water is implicitly present as a continuum dielectric. The first primitive EDL model was proposed about 150 years ago by Helmholtz and is still the starting point of the more sophisticated understanding that has evolved since.[11] In this model, the solid surface is thought to be homogenously charged and the counter ions in water are attracted to the solid surface to offset its electric field, leading to a complete drop of the potential, so that beyond this compact counter ion layer the potential is zero.[11] Later, Gouy and Chapman suggested that the counter ions are adsorbed but not tightly bound to the surface.[12] By applying the Debye–Hückel theory and solving the Poisson–Boltzmann equation, they found that the electric potential shows an exponential decay with increasing distance from the surface.[13,14] Nowadays, the most widely used EDL model is the Gouy–Chapman–Stern model (Figure 1):[15] some ions adsorb to the surface as per the Helmholtz model, forming a compact layer (a.k.a. Stern layer), but not screening the entire electric field; beyond the Stern layer (a.k.a. diffuse layer), the electric potential decays exponentially as the Gouy–Chapman model predicts.[16,17] However, those approximations are problematic since charges are not always uniformly distributed at solid surfaces but may be located on some specific sites, leading to ion specific adsorption that the EDL model is not able to deal with.[18] A more important drawback of EDL models is that they do not take the types of ions into consideration, as a result, the effect of the size and polarization of the ions is missing.

Researchers have developed various experimental techniques, such as X-ray reflectivity (XRR),[19] atomic force microscopy (AFM),[20] scanning tunneling microscopy (STM),[21] nonlinear optical probes including vibrational sum frequency generation (vSFG)[22] and second harmonic generation (SHG),[22] ambient pressure X-ray photoelectron spectroscopy (APXPS)[23] as well as measuring contact angle,[24,25] to study the structure and dynamics of water/solid interfaces. For example, Catalano et al. measured the XRR spectra of water/corundum (001),[26,27] (110),[28] and (012)[29] interfaces and analyzed the electron density profile by fitting the XRR spectra and found that water organization within 1 nm from the solid surface was affected. Experimental studies by vSFG spectroscopy have sought to understand how pH and ions affect interfacial water structures at the alumina[30–33] and silica interfaces.[34–36] However, as most experiments can

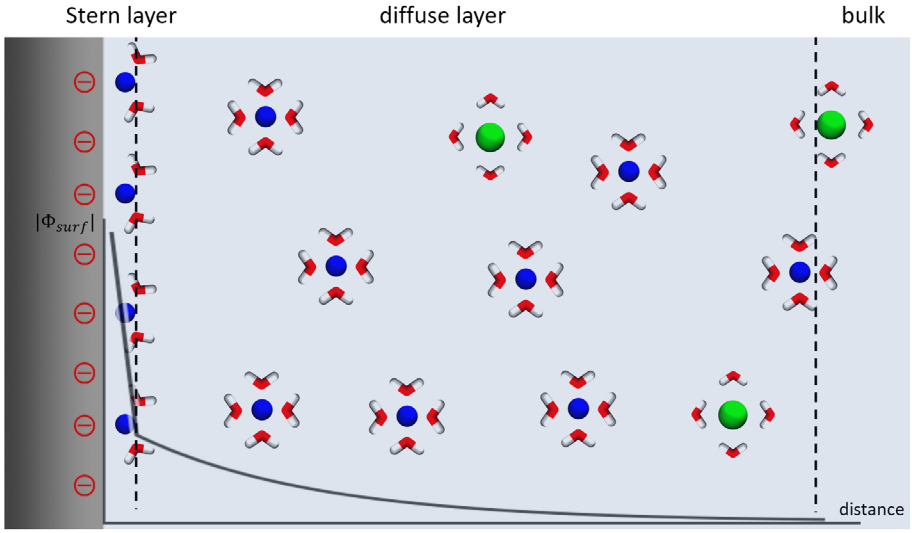

FIGURE 1 A snapshot of a surface following the Gouy–Chapman–Stern model. At the interface, cations are in excess because the mineral surface is negatively charged. Legend: Blue and green balls represent positive and negative ions, respectively; red and white sticks represent the hydration shells of ions

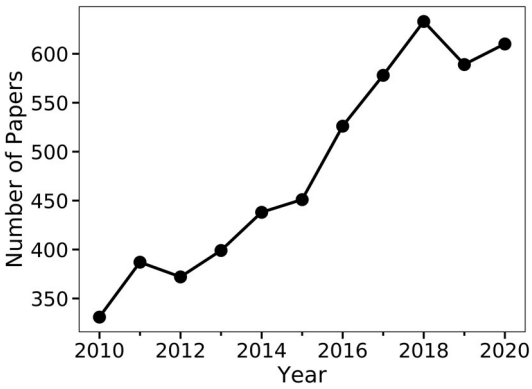

FIGURE 2 Number of articles published since 2010 by searching "water," "interface," and "molecular dynamics simulations" as key words. Source: "Web of Science"

only provide indirect information on the structure of the surface, including the organization of water and solutes at the interfaces, researchers need models and hypotheses to interpret experimental results. However, even models supported by the highest-level calculations are not perfect.

As a result, an alternative approach, namely computational simulation, has grown in recent years (Figure 2) as computational capability has increased. Unlike indirect experimental results that require further hypotheses for interpretation, simulations provide straight-forward microscopic structural information, i.e., the positions and velocities of each atom in every time step. With the help of easy-accessed visualization tools, researchers can observe chemical and physical processes at interfaces as watching movies.[37] Computational simulations are good at handling energy-related properties, for example, calculating the potentials of the mean force of adsorbed molecules, or searching for transition states during catalyzed reactions, which are difficult to measure by experimental techniques. The analysis of simulation results also becomes convenient with the help of Python, an interpreted, high-level programming language, and its libraries created by various developers.[38–40]

Several reviews discussing molecular dynamics (MD) simulations of water/oxide interfaces have been published. Bluhm et al.'s review about water at various interfaces, such as water/metal, water/oxide, and other water/hydrophobic surfaces, featured results from both experiments and simulations.[1] Striolo et al. reviewed water/silica, water/alumina interfaces in 2011,[41] and water/carbon interfaces in 2016.[42] YazdanYar et al. published a review discussing the adsorption of biological molecules at water/rutile surfaces.[43]

In this review, after a basic introduction to the principles of MD simulations, we will focus on recent studies of water/silica, water/alumina, water/TiO_2 and other mineral oxide interfaces. This review is "application-oriented", showcasing what MD simulations are able to do, what chemical scenarios can be investigated and how simulations are helpful to interpret experimental observations, such as revealing microscopic structural information of interfacial water or surfaces-adsorbed solutes, calculating the free energy of chemical reactions, assigning vibrational modes to certain species and more. At the end of the article, we will discuss promising future directions including the application of neural-network potentials.

2 | PRINCIPLES OF MOLECULAR DYNAMICS SIMULATIONS

MD simulations can be used to calculate expected values of observables for macroscopic systems, given that the microscopic interactions are known. This approach relies on the ergodic hypothesis, i.e., the ensemble average of the observations ($<A>$) is equal to the time average calculated using the momentum $\boldsymbol{p}$ and the coordinates $\boldsymbol{q}$ from the trajectories of simulations:

$$<A> = \int \rho(\boldsymbol{p},\boldsymbol{q}) A(\boldsymbol{p},\boldsymbol{q}) d\boldsymbol{p} d\boldsymbol{q} = \frac{1}{T}\int_0^T A[\boldsymbol{p}(t),\boldsymbol{q}(t)]dt \quad (1)$$

where, $\rho(\boldsymbol{p}, \boldsymbol{q})$ is the probability density of state $(\boldsymbol{p}, \boldsymbol{q})$:

$$\rho(\boldsymbol{p},\boldsymbol{q}) = \frac{e^{-\beta H(\boldsymbol{p},\boldsymbol{q})}}{\int e^{-\beta H(\boldsymbol{p},\boldsymbol{q})} d\boldsymbol{p} d\boldsymbol{q}} \quad (2)$$

One crucial aspect of simulations is calculating the position of all atoms as a function of time and this is done by integrating the equation of motion, typically using a numerical procedure known as the Verlet algorithm[44]:

$$r_i^{(\alpha)}(t+\Delta t) = 2r_i^{(\alpha)}(t) - r_i^{(\alpha)}(t-\Delta t) + \frac{f_i^{(\alpha)}(t)}{m_i}\Delta t^2 + O\left(\Delta t^4\right), \tag{3}$$

where, $r_i^{(\alpha)}(t)$ and $f_i^{(\alpha)}(t)$ is the α Cartesian component of the position and force vector, respectively, of the *i*th particle at time *t*.[45,46] Depending on how this force is calculated, simulations are referred to as classical MD or ab initio MD (AIMD).

In classical MD, electrons are not always treated explicitly and interactions between atoms can be modeled heuristically using simple analytic functions of the atoms' positions. In non-reactive MD simulations, chemical bonds are defined in the initial configurations and cannot break or form during simulations. The potential of interactions is decomposed into bonded interaction and non-bonded interaction[47]:

$$U_{\text{total}} = U_{\text{bond}} + U_{\text{angle}} + U_{\text{dihedral}} + U_{\text{vdW}} + U_{\text{Coulomb}}, \tag{4}$$

the first three terms are bonded interactions, including bond stretching, angle bending, and dihedral torsional interactions:

$$U_{\text{bond}} = \sum_{\text{bonds}\, i} k_i^{\text{bond}}(r_i - r_{i0})^2, \tag{5}$$

$$U_{\text{angle}} = \sum_{\text{angles}\, j} k_j^{\text{angle}}(\theta_i - \theta_{i0})^2, \tag{6}$$

$$\text{U}_{\text{dihedral}} = \sum_{\text{dihedral}\, m} \begin{cases} k_m^{\text{dihe}}[1 + cos(n_m\phi_m - \gamma_m)], n_m \neq 0 \\ k_m^{\text{dihe}}(\phi_m - \gamma_m)^2,\ n_m = 0 \end{cases}. \tag{7}$$

The last two terms in Equation (4) are non-bonded interactions, including the van der Waal's interactions (using the Lennard–Jones 6–12 form) and electrostatic interactions, respectively:

$$U_{\text{vdW}} = \sum_i \sum_{j>i} 4\epsilon_{ij}\left[\left(\frac{\sigma_{ij}}{r_{ij}}\right)^{12} - \left(\frac{\sigma_{ij}}{r_{ij}}\right)^{6}\right], \tag{8}$$

$$U_{\text{Coulomb}} = \sum_i \sum_{j>i} \frac{q_i q_j}{4\pi\epsilon_0 r_{ij}}. \tag{9}$$

The parameters in these equations are determined empirically. As a result, the accuracy of simulations depends crucially on the choice of force field parameters but developing accurate and convenient models is a challenge to researchers. One interesting example is water[48,49]: fixed charge models, either the TIP5P model with fictitious particles modeling electrons lone pairs, or the SPC/E model with particles representing only the atoms, cannot reproduce the structure of the Na^+–water complex well.[50]

Reactive force fields, including ReaxFF,[51] the modified embedded atom method (MEAM),[52] or charge-optimized many-body (COMB),[53] have also been developed and widely used for water/solid interfaces.[54] The energy of ReaxFF is similar to non-reactive force fields with additional terms:

$$U_{\text{total}} = U_{\text{bond}} + U_{\text{angle}} + U_{\text{dihedral}} + U_{\text{vdW}} + U_{\text{Coulomb}} + U_{\text{over}} + U_{\text{specific}}, \tag{10}$$

the U_{over} is penalty for overcoordination and $U_{specific}$ is usually 0 unless in special cases.[55] In ReaxFF, methods for calculating each term in Equation (10) are different from Equations (5)–(9); for example, when calculating

bonded interactions, the concept "bond order," a differentiable property based on atoms' positions, is introduced.

In AIMD, the nuclei are still treated classically, while the forces acting on them are calculated by solving the Schrödinger equation for the electrons: $\hat{\boldsymbol{H}}|\boldsymbol{\Psi}>=\boldsymbol{E}|\boldsymbol{\Psi}>$. This cannot be solved exactly and thus most AIMD simulations are carried out at the density functional theory (DFT) level. Instead of calculating the electron ground state at every step, the Car–Parrinello (CP) approach propagates the electron orbitals by introducing a fictitious mass term to the Lagrangian:

$$L_{\mathrm{CP}}=\frac{1}{2}\sum_{I}M\dot{R}_{I}^{2}+\frac{\mu}{2}\sum_{i}<\dot{\Psi}_{i}\,|\,\dot{\Psi}_{i}>-E(R,\Psi)+\sum_{ij}\lambda_{ij}\left(<\Psi_{i}|\Psi_{j}>\delta_{ij}\right), \tag{11}$$

where the first term is the kinetic energy of nuclei, the second term is the fictitious kinetic energy of electrons, the third term is the Kohn–Sham energy and the last term is the orthogonality constraint of orbitals.[56,57] When $\mu \rightarrow 0$, the CP dynamics approaches Born–Oppenheimer MD.

Historically, MD simulations were introduced in 1950; early simulations were used to study simple systems, such as hard disks (1957)[58] or Lennard Jones particles (1964).[59] The first MD simulation of bulk water was reported in 1971.[60] These seminal simulations used classical MD but those systems only contain about several hundred atoms, and were run for picoseconds due to the limitations of computational resources of that time. Nowadays, the time and length scales of classical MD simulations can reach billions of atoms and milliseconds, respectively.[61,62] As for AIMD, CPMD was introduced in 1985[56]; due to the huge cost of electronic structure calculations, typical AIMD simulations involve hundreds of atoms and time-scales of picoseconds. Finite size effects and limited sampling of the trajectory lead to large uncertainties in the results. However, a major advantage of AIMD is that it can properly handle chemical reactions such as proton transfer,[63] catalysis,[64] and water dissociation[65,66] at interfaces.

MD simulations generate trajectories with conserved energy and momentum; if the volume of the simulation box is also fixed, the simulations are called constant-NVE ensemble (or microcanonical ensemble). However, physical processes in other ensembles, such as NVT, NPT, or even μVT are more interesting and realistic to laboratory conditions. Thanks to several algorithms, such as the Nose–Hoover thermostat[67–69] and the Martyna–Tuckerman–Tobias–Klein algorithm,[70] which make use of extended Lagrangians, simulations of NVT and NPT ensembles can be performed as well.

3 | WATER/SILICA INTERFACES

Silicon oxide is one of the most ubiquitous minerals on the earth and its interaction with water has been investigated by both experimental measurements and MD simulations.[71] Silica surfaces are also involved in many crucial chemical reactions that affect the earth and life,[72] such as the immobilization of CO_2[73,74] and the catalysis of polymerization of amino acids.[75] Silica has multiple forms, including amorphous (in many SHG and SFG experiments researchers use fused silica)[76] and crystalline (quartz).[22] In nature, silica exists in the form of quartz, the second-most abundant mineral on Earth behind feldspar.[77] Although the primary component of silica or quartz is SiO_2, the surface is active to water which reacts providing surface OH groups that show acid–base behavior. Experimental SHG measurements suggest that the pK_a of 19% of the silanol groups is 4.5 and the pK_a of the other 81% is 8.5.[78] The α-quartz (001) surface is also terminated with silanol groups that show two major orientations: OH vector is perpendicular to the surface plane ("out-of-plane") or parallel to the surface plane ("in-plane").[79] In this review, we will discuss several topics about water/silica interfaces, such as ion adsorption, acid dissociation and solid dissolution.

3.1 | Ion adsorption

The point of zero charge (PZC) of silica is in the pH range 2–4,[78] indicating that in ambient conditions (near pH = 7), silica surfaces will release protons and become negatively charged. Traditional EDL theories predict an interfacial electric field profile that points into the solid and exponentially decays into the solution. Interestingly, exceptions are also observed, which is not surprising because in the oversimplified EDL theories many factors such as the charge

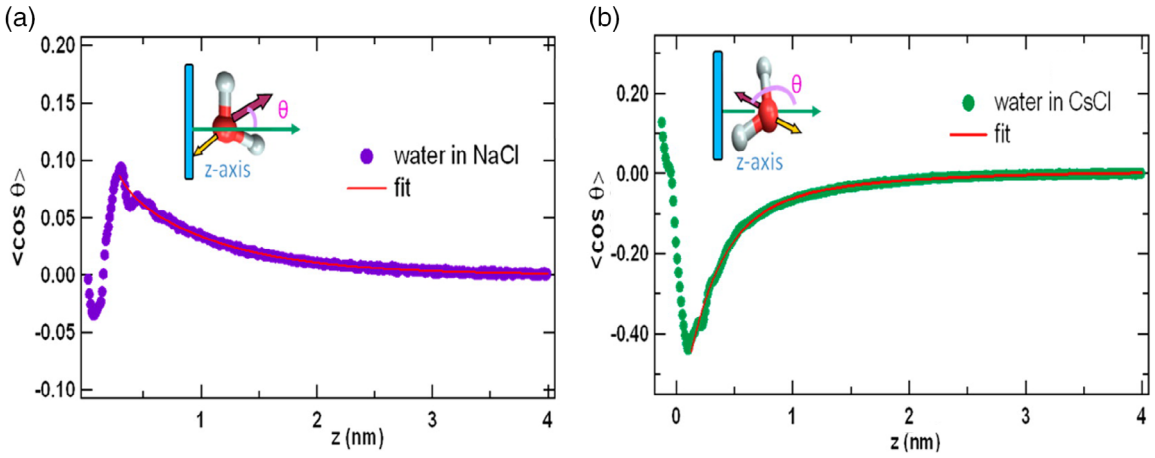

FIGURE 3 Influence of ions on water orientation at the water/silica interface. θ is the angle between the opposite of the water dipole and silica surface normal. The silica surface is negatively charged. (a) after adding NaCl, the surface potential and <cos θ> in the diffuse layer become positive (oxygen close to the surface). (b) CsCl follows the Gouy–Chapman–Stern model. The surface potential and <cos θ> in diffuse layer remain negative (hydrogen close to the surface). Reprinted with permission from Ref. 18. Copyright (2014) American Chemical Society

distribution at the surface and the type of ions are neglected. One example is provided by Dewan et al. who carried out classical MD simulations of amorphous silica/water interfaces to understand how different charge densities, that mimic different pH environments, affect water structure and ion accumulation in the presence of NaCl or CsCl.[18] They also investigated how the charge localization (heterogeneous or uniform distribution) on the surface affects ion adsorption and water organization.[18] Simulations show that, when the surface charge is localized on SiO^- groups, specific adsorption is so strong that when the bulk concentration of Na^+ is high (0.5 M in their work), Na^+ adsorption makes the surface charge positive and reverses the water orientation (described by the opposite of the water dipole) in the diffuse layer, making it point away from silica surface. In contrast, Cs^+ does not directly bind to the surface and follows the Gouy–Chapman–Stern model (GCS) model (Figure 3). Such surface charge reversal is also reported in other works and it is definitely beyond what the EDL or Gouy–Chapman–Stern model can predict.

Another weakness of EDL theories is that solid surfaces are treated as a homogenous charged plane, which is not realistic because ions may prefer to adsorb to specific positions. For example, Hocine et al. calculated the potential of mean force (PMF) of cation adsorption and obtained a similar result to Dewan et al.,[18] finding that Li^+ has a strong adsorption affinity but that Cs^+ is repelled by the surface.[80] The major adsorption mode for Li^+ is to directly bind to deprotonated silanol groups ($Si–O^-$) and such a binding mode is missing in EDL theories. Based on such observations, Hocine et al. proposed that the Stern layer is not a continuous layer but consists of some discrete contact ion pairs at the surface, for example, $SiO^-...M^+$. As a result, predicting ion behavior simply based on its distance to the surface is not appropriate. These examples demonstrate the weakness of EDL theories at mean field levels and the necessity for more detailed structural information, which AIMD simulations are able to provide.

Interactions between the silanols that cover the surface of SiO_2 and ions are well studied for better understanding of geochemistry using both classical and ab initio MD simulations. In classical MD simulations, ion adsorption at different pH is usually studied by modifying the model of solid surface, typically changing the surface charge density or removing protons.[81–83] Not surprisingly at higher pH, when the surface contains more negative charge associated with deprotonated silanol sites, cations have higher accumulation in the Stern layer,[82,84] and the diffusion of these ions is slower than in the bulk. Such observation could be one evidence that ions in the Stern layer are tightly bound to solid surface but are still able to move; water diffusion is also slower at the interface and even slower near deprotonated silanols.[81] In addition, ions near deprotonated silanols further decrease water diffusion.[81]

Besides classical MD, AIMD was also introduced to investigate ion adsorption at water/α-quartz interfaces. Pfeiffer-Laplaud et al. studied the adsorption of a single alkali ion and found that Na^+ and K^+ directly bind to the α-quartz (001) surface with partial substitution the solvation shell by surface hydroxyls, through an inner-sphere mechanism, but halides do not have any hydrogen bonds to the surface.[85] DelloStritto et al. investigated the acidic, neutral, and basic water/quartz (101) interfaces with IA, IIA group ions and Cl^-.[86] They found that cations directly bind with the surface and behave differently from the bulk. Specifically, in the presence of a counter-ion Cl^-, the structure makers, Na^+, Mg^{2+} and Sr^{2+}, become structure breakers at the interface; the strongest "structure breaker" cations in bulk water

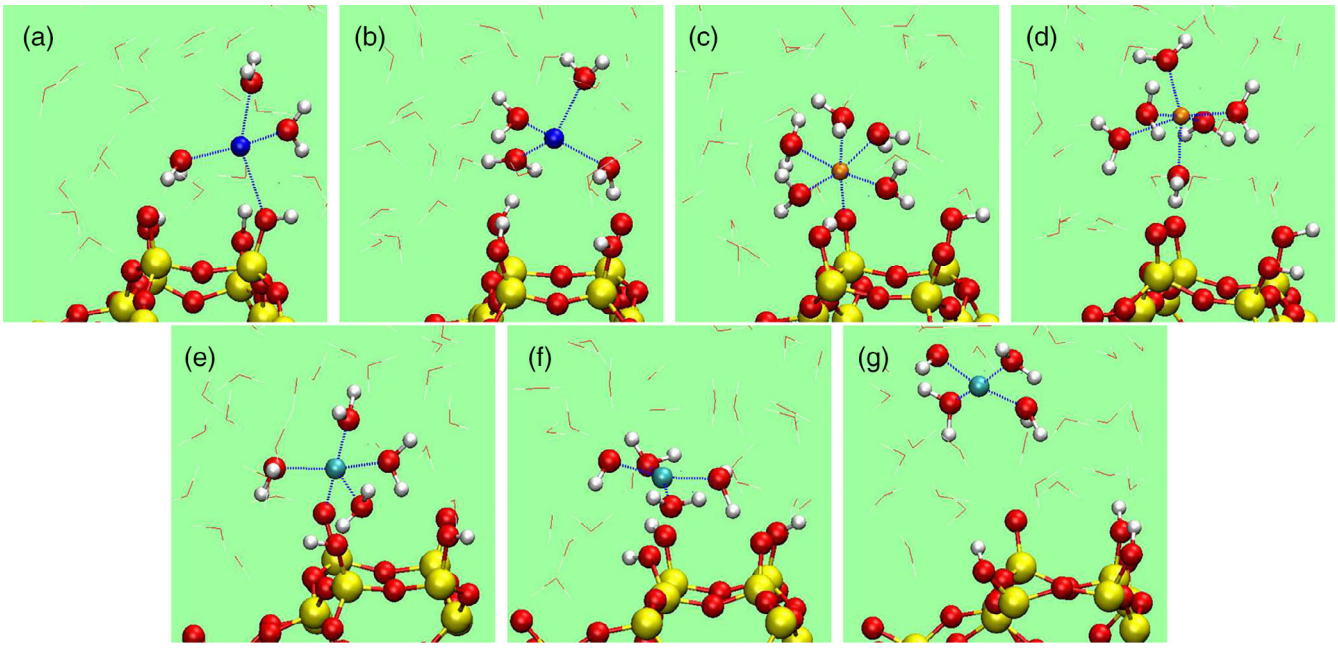

FIGURE 4 Different ion binding modes between ions and the β-crystabolite (001) surface. Yellow, red, white, blue, orange and green balls represent Si, O, H, Na, Mg, and Cu atoms(ions), respectively. (a,b) Na^+ binding modes, (c) Mg^{2+} directly binds to the surface, (d) Mg^{2+} with completed hydration shell. (e) Cu^{2+} binds to the surface, (f,g) $Cu(OH^-)(H_2O)_3$ complex ion. Reprinted with permission from Ref. 87. Copyright (2018) American Chemical Society

are the strongest "structure maker" ions at the interface. These results support previous inferences from experimental data and remind researchers that simple bulk classifications of structure maker/breaker do not always carry over to interfaces. Based on these investigations, additional questions can be asked and answered using MD simulations, such as how different surfaces and other anions affect the structure makers/breakers.

Both AIMD and classical MD predict strong Na^+ adsorption at quartz/water interfaces, which is not true for all other silica surfaces. Leung et al. calculated the PMF of cation adsorption with the solvation shell onto a partially deprotonated β-crystabolite (001) surface (Figure 4), a different crystal phase of SiO_2, by umbrella sampling using AIMD.[87] They found that Na^+ does not bind to that surface. Mg^{2+} can bind to the surface either directly, in the form of $Mg(H_2O)_5(SiO^-)$, or via its intact hydration shell. Direct binding is more favored by about 0.2 eV. Interestingly, the surface SiO^- will grab a proton from the hydration shell of Cu^{2+}, forming a $Cu(OH^-)(H_2O)_3$ complex ion. As a result, the authors proposed that in future CMD simulations, a Cu^{2+}-OH^- based model should be used. Although AIMD is much more expensive than classical MD, it is useful and necessary if the hydration shell of ions is able to release protons.

Adsorbed cations affect surface silanol properties as well. In the presence of cations, the intra-surface H-bond network is weakened, accelerating the switching of silanols between "in-plane" and "out-of-plane" modes, which is rarely observed at neat interfaces on typical AIMD timescales.[85] In their later work, Pfeiffer-Laplaud et al. studied a cation–anion solvent separated pair at the same surface and found that the orientation and bond-length of the surface OH groups are more affected and that intra-surface H-bonds are more weakened by such an ion-pair than by a single ion.[88]

In addition to the works mentioned above, there are other studies investigating ion adsorption at interfaces,[89] including organic molecule ions.[90] Other than simulations with only one type of ion-pair, Döpke et al. carried out simulations of water/silica interfaces with the NaCl–$CaCl_2$ mixture and found that Na^+ shows more preferential adsorption to silica surface than Ca^{2+} because Na^+ has a less tight hydration shell and the surface structure adsorption site does not match the hydration shell of Ca^{2+}.[91]

3.2 | Acid dissociation

There are several interesting pK_a related questions about interfaces: how do surfaces affect the water pK_a, what is the pK_a of the surface OH groups, how do adsorbed solutes affect the surface pK_a and how do surfaces affect the pK_a of

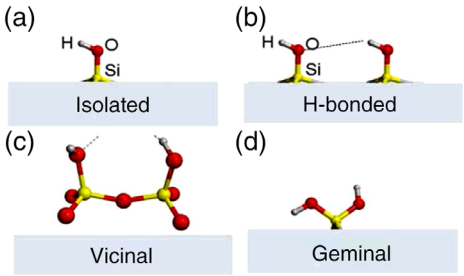

FIGURE 5 Classification of silanols on amorphous silica surfaces. "Isolated" silanols are not hydrogen bonded with other silanols; "vicinal" silanols share one common oxygen atoms and "geminal" silanols have two OH groups connected with one silicon atom. Reprinted with permission from Ref. 101. Copyright (2015) American Chemical Society

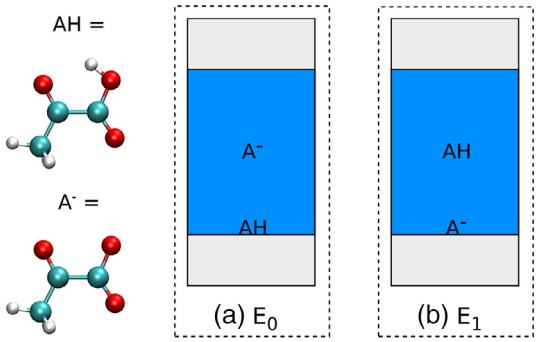

FIGURE 6 The calculation of ΔpK_a of pyruvic acid at an interface. The structures are the protonated acid (HA) and the deprotonated ion (A^-). (a) Initial state with HA at the surface and A^- in the bulk. (b) Final state with A^- at the surface and HA in the bulk. Reprinted with permission from Ref. 102. Copyright (2018) American Chemical Society

solutes at the interface. Answering such questions is quite challenging due to the complicated environment of interfaces and even the value of the water pK_a at water/air interfaces, possibly the simplest surface, is still controversial because some MD simulations show that water/vapor interfaces are acidic,[92–95] but the opposite result that such interfaces are basic has also been reported.[96–98] Nevertheless, significant advances related to the acid/base chemistry of water/silica interfaces have been made with the help of MD simulations.

The simplest example is the pK_a calculation of hydroxylated α-quartz (0001) surface OH groups as there is only one type of silanol with two orientations; "out-of-plane" silanols are reported to have a lower pK_a (5.6) than "in-plane" silanols (8.5).[99] When an alkali–halide ion pair is placed at the interface, the cation will bind to the oxygen atom of the silanols, stabilize the OH bond and prevent deprotonation.[100]

The pK_a of amorphous silica silanols is more complicated. Using free energy perturbation, Pfeiffer-Laplaud et al. identified and calculated the pK_a of four types of silanols on silica surfaces: isolated, H-bonded, vicinal, and geminal; the terminal group of the former three is SiOH and that of the last one is $Si(OH)_2$ (Figure 5).[101] They found that convex geminal and vicinal silanols have strong acidity with a pK_a value about 2–3, while the isolated and concave germinal species have much higher pK_a (9–10). Such bimodal acidity has already been observed by SHG experiments[78] and with the help of AIMD simulations researchers can identify its microscopic origin.

A more interesting question, perhaps, is understanding how interfacial environments affect the acid/base chemistry of species nearby, such as the pK_a of a solute molecule. This topic has a close relationship to heterogeneous catalysis, including amino acid condensations reactions near water/silica interfaces. Parashar et al. constructed water/α-quartz (0001) interfaces with two pyruvic acid molecules (Figure 6), one at the surface in a protonated state (HA) and the other one in the bulk in the form of a deprotonated ion (A^-).[102] Using the free energy perturbation method,[103] they calculated the Helmholtz free energy difference to move the proton from the HA molecule at the surface to the A^- in the bulk. They found that at the interface, the acidity increased due to the stabilization of A^- by surface OH groups and interfacial water. The design of this work is ingenious since it only calculated the pK_a differences of an acid at the surface and in the bulk, instead of calculating absolute pK_a values.

3.3 | Simulations of vibrational spectra

Besides analyzing chemical structures and calculating free energies, MD simulations can also help interpret experimental vibrational spectra, such as IR and Raman. For water/solid interfaces, nonlinear optics, such as vSFG and SHG are

intensively used because they are sensitive to non-symmetric environments that interfaces naturally possess.[22] Usually, vSFG spectra can be decomposed into $\chi^{(2)}$ and $\chi^{(3)}$ contributions, arising from interfacial region and bulk water, respectively.[104] The $\chi^{(2)}$ contribution is determined from the autocorrelation function of the molecular dipoles and polarizabilities.[105]

Since the silica surface is charged at pH 7, it has been widely used as a model of charged surfaces by combining MD simulations and experiments. Gaigeot et al. calculated the vibrational density of states of interfacial OH groups (both from water and silanols).[79] They found that the H-bonds that water molecules donate to the "in-plane" silanols (OW-HW...OSi) are weak and contribute to vibrations in the 3300–3600 cm^{-1} range. By carefully calculating the vSFG spectra of water in different layers close to interfaces, Pezzotti et al. proposed a new definition of the electric double layer. To be specific, the boundary of the Stern layer (in their work it is called the "binding interfacial layer") can be identified because its properties, such as water density profile and hydrogen bond profile, are distinct from bulk water and their vSFG spectra are surface type dependent. However, the hydrogen bond structure in the diffuse layer behaves similarly to bulk water except for the net orientation caused by the interfacial electric field. As a result, the vSFG signals of water in diffuse layers of water/quartz and water/air interfaces are similar.[106] This work is a demonstration that water in the diffuse layer follows the assumptions of EDL theories that water is aligned by a homogenous electric field. It will interesting to see whether the diffuse layer of other aqueous interfaces follow this pattern.

The combination of vSFG and simulations provides detailed microscopic structural information and is helpful for researchers to understand the behavior of water interfaces, not limited to water/silica interfaces.[105,107–110] One interesting question at charged water/solid interfaces is the separation of the second-order ($\chi^{(2)}$) and the third-order ($\chi^{(3)}$) contributions of vSFG spectra; the latter one comes from the static electric fields of charged interfaces. Several experimental attempts for such separation have been reported by changing the pH or ion concentrations.[111,112] However, those methods are not perfect because the surface charge state and water structures in the compact layer are also affected, leading to the change of $\chi^{(2)}$ signal as well.[113–115] By designing MD simulations containing water between two charged silica surfaces, modifying the charge density on the surfaces and calculating how the water responded to this electric field, the corresponding $\chi^{(3)}$ contribution

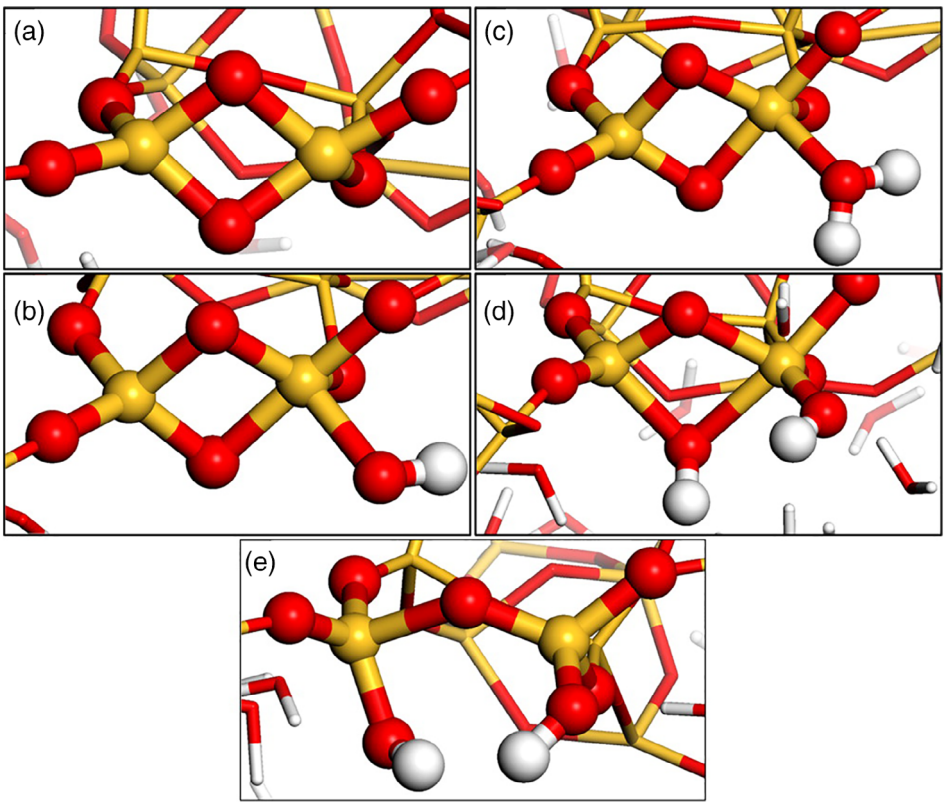

FIGURE 7 The mechanism of how strained silica become unstrained silica. (a) Strained silica, the initial state. (b–d) Intermediate defect structures. (e) Unstrained silica, the final state. Reprinted with permission from Ref. 118. Copyright (2016) American Chemical Society

could be extracted.[104] This procedure helps researchers understand the $\chi^{(3)}$ effects near charged water/solid interfaces and such a decomposition can be used to extract the $\chi^{(2)}$ component from vSFG spectra to investigate the interfacial structure.

The preceding discussions focused on perfect solid silica surfaces. However, water/silica interfaces are not always stable, especially in high pH solutions,[116] and the dissolution (or degradation) can also be studied by MD simulations.[117] Using both classical MD with ReaxFF and AIMD simulations, Rimsza et al. calculated the first step of silica dissolution, the breaking of strained silica and the formation of unstrained silica (Figure 7).[118] First, a water molecule adsorbs onto an external Si atom of a strained silica site and releases a proton (Figure 7(a–c)); next, another proton comes to the bridging oxygen, leading to the rupture of the Si–O bond (Figure 7(d,e)). Simulations also provide the time scale of such reactions.[118] In their later work, they also studied the evolution of the silica gel region between bulk water and bulk silica solid.[119] Since the dissolution of silica is usually neglected when studying water/silica interfaces, these works provide useful information regarding solid dissolution and may help researchers improve their design of experiments to avoid/promote silica dissolution.

4 | WATER/ALUMINA (ALUMINUM OXIDE) INTERFACES

Aluminum is the third most abundant element on earth after oxygen and silicon, and mostly exists in the form of oxides due to its high reactivity. However, water/alumina interfaces are less understood than water/silica interfaces in spite of their important roles in ion adsorption and catalysis. Alumina has wide industrial applications,[120] for example, γ-Al_2O_3 can be used as the support for catalysts.[121,122] We focus on α-Al_2O_3 because it is the most thermodynamically stable phase; the coordination number of aluminum is 6 in bulk α-alumina, forming an octahedron and that of oxygen is 4, forming a tetrahedron. The fully hydroxylated, charge neutral water/α-Al_2O_3 interface has been studied by several groups focusing on interfacial water structures and dynamics.[26,41,84,123,124] Particularly, the vSFG of water/alumina (0001) and $(11\bar{2}0)$ interfaces under various pH in the presence of monovalent ions has been measured to estimate the structures of interfacial water and hydrogen bonds.[30,33] The α-alumina (0001) surface is flat, containing only one type of aluminol Al_2OH, but the $(11\bar{2}0)$ surface is rough and complicated, containing AlOH, Al_2OH, and Al_3OH groups with different heights (Figure 8).

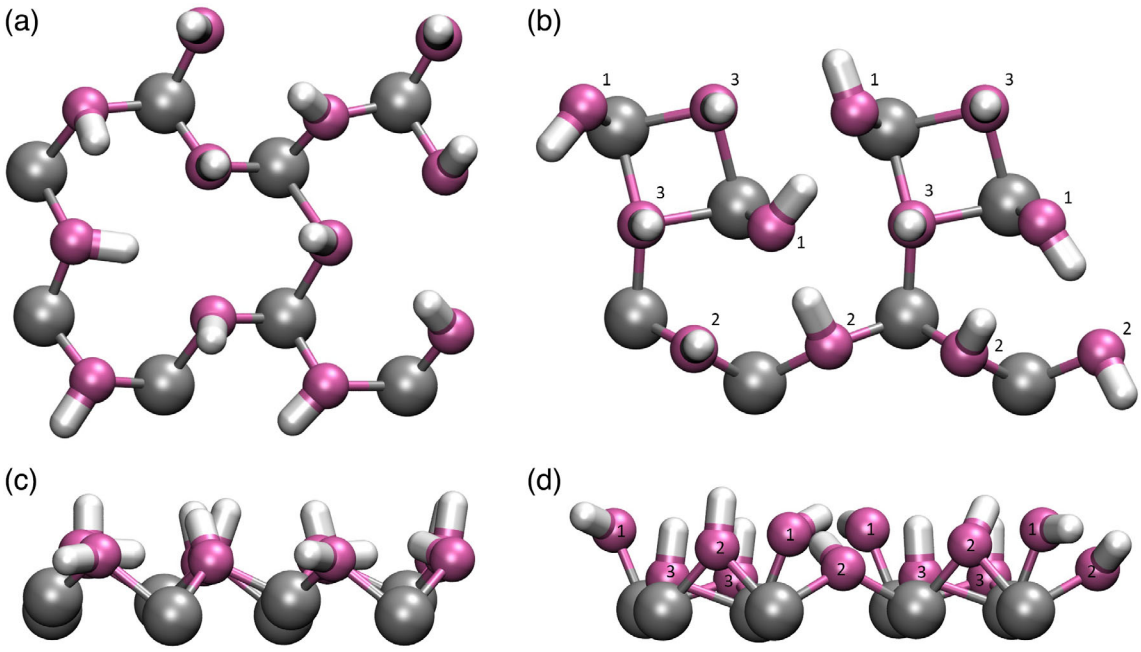

FIGURE 8 The structure of α-alumina (0001) and $(11\bar{2}0)$ surfaces. Water is not shown for clarity and gray, purple and white color represent aluminum, oxygen and hydrogen atoms, respectively. The top two figures show the top view of (0001) (a) and $(11\bar{2}0)$ (b) surfaces; the bottom two show the side view of (0001) (c) and $(11\bar{2}0)$ (d) surfaces. The numbers in figure (b) and (d) represent how many aluminum atoms are connected with each oxygen, that is, the "x" of Al_xOH. The figures only show one simulation box so the periodic boundary condition is broken

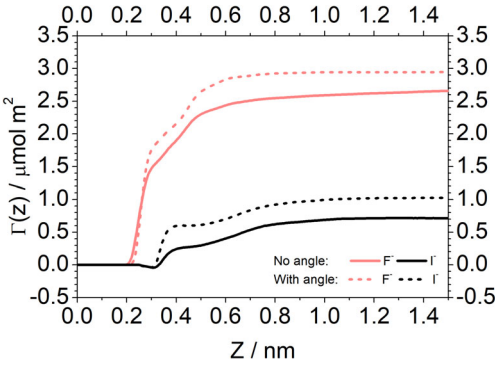

FIGURE 9 Surface excess ions per unit surface area, Γ(Z), profile of F^- and I^- near the water/α-alumina (0001) interface. The counter-ion is Na^+. Comparing to results with the Al-O-H angle bending potential, simulations without it underestimate ion adsorption. Reprinted with permission from Ref. 125. Copyright (2019) American Chemical Society

The impact of ions on water/alumina interfaces has also been investigated by MD simulations. Wang et al. observed unusual ion adsorption onto the water/α-alumina (0001) interface, due to the special pattern of surface OH groups.[125] By comparing the adsorption free energy, they found that in simulations of a single ion, Na^+ has a stronger affinity to the solid surface than halides; in simulations of finite concentration solutions, the affinity of Na^+ decreases and that of halides increases, indicating that adsorbed Na^+ ions promote halide ion adsorption.[125] The adsorbed excess Na^+ can increase water polar orientation and change its dipole direction. As discussed before, such effects cannot be predicted by EDL theories. In addition, ignoring the Al–O–H angle bending term in the potential could cause the underestimation of ion adsorption (Figure 9).[125] Recently the angle bending terms in ClayFF have been improved, leading to a distribution of the orientations of surface OH groups that is in better agreement with DFT simulations.[79,126,127]

AIMD simulations are also applied to calculate and analyze the vibrational spectra of alumina/water interfaces. DelloStritto et al. successfully reproduced the features observed in experimental spectra of the water/α-alumina (0001) interface, namely a peak centered at 3150 cm^{-1} and a higher peak around 3450 cm^{-1},[128] which were previously assigned to water with different coordination numbers.[129] However, both water and "in-plane" aluminols contribute to the 3400 cm^{-1} peak and the latter is usually ignored. Further calculation of the vibrational density of states indicates that "out-of-plane" aluminol vibrations are at higher frequency, between 3600 and 3800 cm^{-1}, unlike the α-quartz (0001) surface whose vibrational density of states of both "in-plane" and "out-of-plane" silanols overlap in a wide region 3000–3800 cm^{-1}.[79] Later, DelloStritto et al. compared the performance of several popular exchange and correlation functionals, including PBE, PBE with Tkatchenko−Scheffler correction (PBE-TS), revised PBE and SCAN meta-GGA functionals; they found that revised PBE has poor performance in reproducing experimental interfacial water structures and vSFG spectra, even though it does well for the water/vapor interface.[108] Spectra predicted by revised PBE show too much blueshift whereas spectra from PBE or PBE-TS have stronger intensity in the low frequency region, indicating that they predicted an overstructured interfacial water as they did for bulk water.[130,131] The meta-GGA SCAN functional,[132] which has provided more accurate description of the structure,[133] dynamics,[134] IR spectra[135] and pK_a[136] of bulk water as well as the solvation structure of Cl^-,[137] outperforms PBE-TS, giving the best interfacial structure, dynamics and vSFG spectra, demonstrating that the SCAN functional can describe interfacial water and the solid surface well at the same time (Figure 10).[131] Interestingly, the spectrum of the α-alumina $(11\bar{2}0)$/water interface shows more redshift than the less corrugated (0001) interface while water at the (0001) interface has longer H-bond lifetimes and a larger order parameter. As a result, concepts such as "strong H-bonded", "ordered", "redshifted" and "ice-liked" are correlated, but they are not equal and observing one behavior does not guarantee the others. Thus, we should be careful when using these concepts.

The vSFG of the alumina (0001) surface was also calculated by Melani et al. with simplified parametrized velocity–velocity autocorrelation function methods and they proposed a similar interpretation as DelloStritto et al.[138] These works provide a well-defined paradigm to analyze vSFG spectra using AIMD simulations: running simulations with advanced density functionals, such as the SCAN functional, then calculating the vSFG spectra of the system and its components. By carefully comparing simulation results and experimental measurements and assigning experimental peaks, more microscopic structure information can be revealed to advance our understanding of water/solid interfaces.

Besides vSFG, XRR is also used to study the water/α-alumina (0001) interface. The effective electron density can be obtained by fitting the XRR and compared with that calculated from MD simulations.[26,139] The experimental and simulated results were qualitatively similar, but quantitatively different (Figure 11), indicating that an improvement of current density functionals is still required, especially the ones with moderate cost that could be used for AIMD simulations.[26,139]

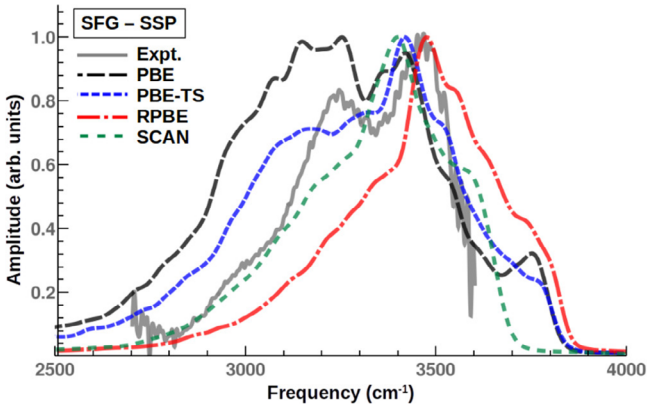

FIGURE 10 Comparison of vSFG spectra of the water/α-alumina (0001) interface from experiments and AIMD simulations. The spectrum predicted by SCAN agrees best with experiments in this work. Spectra from PBE or PBE-TS overestimate intensities at low frequency while features at low frequency are missing in RPBE. Reprinted with permission from Ref. 131. Copyright (2019) American Chemical Society

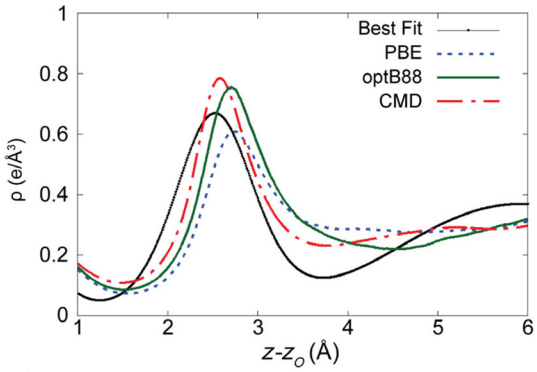

FIGURE 11 Comparison of experimental and simulated electron density profiles of the water/α-alumina (0001) interface. The "z–z_0" is the distance of Z direction (surface normal) and 0 is set to the surface outmost oxygen plane. Black curve ("best fit") is the fitted electron density from XRR measurements. Blue ("PBE") and green ("optB88") curves are results directly calculated from AIMD simulations using different functionals. Red curve ("CMD") is results from classical simulations. Reprinted from Ref. 139

As mentioned above, alumina draws less attention than silica and many important questions still puzzle researchers. One example is the pK_a of the octahedral Al_2OH group, which is the only type of hydroxyl group on the alumina (0001) interface, reported as 16.6 by one source,[79] while the pK_a of water/gibbsite (0001) reported as 22,[140] both determined using the BLYP functional. Gibbsite is one polymorph of $Al(OH)_3$ whose (0001) surface has similar octahedral Al_2OH groups as alumina (0001). However, experimental measurements using potentiometric titration report the pK_a of Al_2OH as 12.5.[141] The reason of such discrepancy between experiments and simulation is unknown and requires more investigation. What is more, a bigger problem is that the experimental pK_a is smaller than that of water, indicating the surface deprotonates in basic solutions but all simulation results predict that the surface cannot release any protons in water.[140] Interestingly, hematite (0001) surface is similar to alumina (0001) and the predicted pK_a of Fe_2OH by AIMD is 21.7, comparable with Al_2OH, but much higher than the value predicted by the valence bond model (about 12).[142] The pK_a of SnO_2 is consistent with experimental PZC measurements.[143] Understanding disagreements between simulations and experimental measurements is crucial to model the interface in acidic or basic solutions because the surface protonation state, surface charge density, and interfacial water orientation are mainly determined by the surface pK_a.

5 | WATER/TIO_2 INTERFACES

Titanium oxide is widely used in white pigments, photocatalysts, electrochemical devices, and biocompatibility materials.[144] Several reviews focusing on TiO_2 surfaces or water/TiO_2 interfaces have been published in the past few years.[145–147] Common TiO_2 forms occurring in nature are rutile, anatase and brookite. Rutile (110) is the most stable facet and has been the most widely studied.[148]

5.1 | Water adsorption

The simplest scenario related to water/TiO_2 interfaces is the pure water adsorption onto the perfect, defect-free solid surface, which has been studied by the combination of experimental phase-sensitive vSFG and AIMD simulations. The

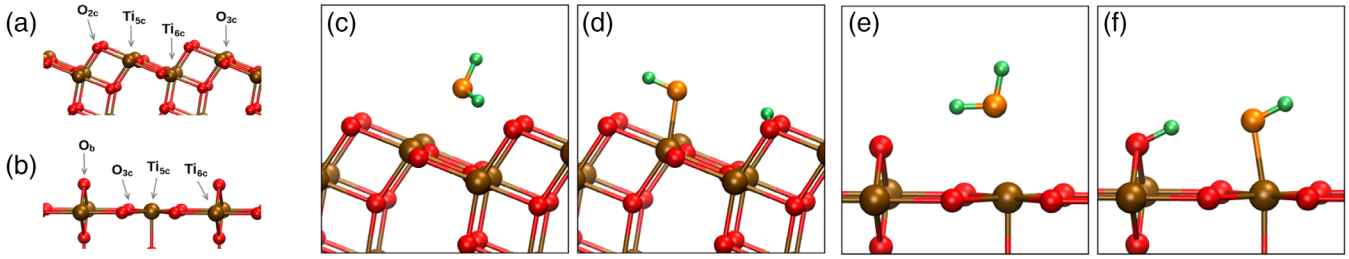

FIGURE 12 Water dissociative adsorption on TiO_2 surfaces: (a) the structure of anatase (101) and (b) rutile (110) surfaces with atom labels; (c) before and (d) after water dissociation at the anatase (101) surface; (e) before and (f) after water dissociation at the rutile (110) surface. Reprinted with permission from Ref. 151. Copyright (2017) American Chemical Society

vibrational spectra have been computed and both Hosseinpour et al.[149] and Andrade et al.[150] observed a positive peak at 3100 cm^{-1}, assigned to "physisorbed" water that donates a strong H-bond to the surface, and a negative peak at 3400 cm^{-1}. However, the origin of feature at 3400 cm^{-1} is under debate. Hosseinpour et al. proposed the concepts "chemisorbed" and "physisorbed" water; the former is dissociated water forming a covalent OH bond with the surface five coordinated Ti atoms and the latter remains as an intact water molecule. In Hosseinpour et al.'s work, the feature at 3400 cm^{-1} is assigned to "chemisorbed" water molecules,[149] while in Andrade et al.'s work, after water dissociative adsorption, the signal at 3400 cm^{-1} decreased comparing to non-dissociated simulations, because such dissociation perturbed water in the first layer.[150]

The "chemisorbed" water is also reported in other simulations of water/anatase (101) and water/rutile (110) interfaces using a reactive force field.[151] Water first contacts with 5-coordinated Ti atoms, dissociates leaving hydroxyl groups that form $Ti_{5c}OH$ like structures. The resulting H^+ moves to the nearest 2-coordinated surface oxygen (O_{2c} for anatase and O_b for rutile, Figure 12). All O_{2c}/O_b sites are covered by H^+ but only half of the Ti_{5c} sites are terminated by OH^-. The coverage of Ti_{5c} for anatase (101) is higher than that of rutile (110), leading to a higher positive surface potential of rutile (110) than that of anatase (101). The diffusion constant of water near those interfaces is about 2 orders of magnitude slower than the bulk, indicating strong water–interface interactions but the average interfacial hydrogen bonds strength and lifetime do not increase significantly. One weakness of this simulation is that the IR spectrum predicted by ReaxFF is less accurate than expected, indicating that fast classical simulations may not be able to reproduce all the properties of the studied systems.

Water dissociation is also observed at the brookite (210) interface and interestingly, ions, such as K^+ and Cl^-, are found to promote water dissociation and increase surface hydroxylation, that is, more than 30% of surface groups are hydroxylated when KCl is present, comparing to less than 20% in pure water.[152] Previous research has shown that the hydroxylation of the TiO_2 anatase surface can enhance the photocatalytic efficiency for water splitting.[153] Since the carbonate ion can enhance hydrogen evolution at the $K_4Nb_6O_{17}$ surface,[154] it will be exciting if ions can further increase the photocatalytic efficiency on TiO_2 or other surfaces.

According to the works discussed above, simulations have enabled a clearer picture about the microscopic nature of (pure) water/TiO_2 interfaces to emerge. Some TiO_2 surfaces are superhydrophilic due to strong interactions with both "physically" and "chemically" adsorbed interfacial water. The chemical adsorption, or dissociative adsorption of water, can also happen at water/TiO_2 interfaces, making the surface OH terminated. Since electrochemical catalysis is one of important applications of TiO_2, preliminary knowledge of water adsorption on the TiO_2 is essential to inspire better materials design.

5.2 | Electrochemical applications

Since 1972, when Fujishima and Honda discovered the photocatalytic power of TiO_2,[155] designing high efficiency materials for water splitting or hydrogen generation to overcome the energy crisis has become one of the most popular areas in scientific research. Many MD simulation articles related to this topic have been published in recent years, mainly focusing on the oxygen evolution half-reaction (OER), the rate-determining step at TiO_2 interfaces.[156,157] Valdés et al. proposed the following mechanisms from AIMD simulations of the water/rutile (110) interface for water oxidation,

containing four sequential proton-electron transfer (PET) steps at water/anatase (101) interfaces in the presence of surface-trapped photoexcited holes[157]:

$$*OH_2 + h^+ \rightarrow *OH + H^+ \quad (12)$$

$$*OH + h^+ \rightarrow *O + H^+ \quad (13)$$

$$*O + H_2O + h^+ \rightarrow *OOH + H^+ \quad (14)$$

$$*OOH + h^+ \rightarrow O_2 + H^+, \quad (15)$$

in which the first step is the most difficult. Recently, Li et al. investigated water oxidation on the anatase (101) surface using the hybrid density functional PBE0.[158] Based on the mechanism above, the authors find that the first step requires water adsorption at Ti_{5c} site and release of a proton to create an *OH radical.[158] Next, the proton in the *OH radical leaves, the *O and a surface oxygen together form a bridging peroxo dimer $(O_2^{2-})_{br}$. The last two steps involve a concerted two-electron-transfer pathway, instead of a nucleophilic attack from water that was reported at a rutile surface.[159–161] The authors also state that the lower probability of the two-electron-transfer is the reason for the lower OER performance of anatase compared with rutile.

Stecher et al. calculated the free energy barrier for water oxidation at the rutile (110) interface using quantum mechanics/molecular mechanics (QM/MM) techniques.[162] QM/MM can provide better sampling and overcomes some infinite-size effects due to the limited scale of AIMD simulations. Another improvement of this work is that energy gap is selected as the reaction coordinate instead of common geometric coordinates. The results show that the free energy barrier is 0.2–0.25 eV higher than the rutile band gap, depending on the orientation of the bridge water molecule. Those numbers indicate that OER reactions are not able to happen near the perfect rutile (001) interface. An alternative hypothesis is that defects on the surface promote water dissociation, which has been observed on the rutile (110) surface.[163] Excess electrons can be generated from the defects and their behaviors have been investigated by Selcuk et al.[164] They found that an excess electron at the water/anatase (101) interface can be trapped, forming a stable Ti^{3+}–$O_{br}H$ complex, which facilitates reduction reactions. However, the (001) surface repulses electrons and oxidation reactions are favored. These results are in good agreement with photoemission spectra and the authors proposed that catalytic activity can be tuned by optimizing the ratio of anatase (101) and (001) surfaces. Since catalysis at TiO_2 surfaces is still a hot area, simulations can be used to reveal the mechanisms by quantifying the free energy along reaction coordinates or analyzing the electron behaviors.

5.3 | Biomolecule adsorption

Due to the biocompatibility and biosafety of TiO_2, its applications as implant materials or biosensors are of great interest.[43,165] It is necessary to investigate the interaction between the solid surface and small biomolecules since they are ubiquitous in human beings and some of these interactions could be harmful to patients. Amino acids or short peptides can be chosen as model molecules since they can be a mimic of proteins, the molecules of life.

YazdanYar et al. studied the adsorptions of several single amino acids (Ala, Asp, Lys, Arg, Leu, and Ser) on the negatively charged rutile (110) surface.[166] Using well-tempered metadynamics, they calculated the PMF with respect to two collective variables, the distance between the solid surface and center of amino acids' backbone or side group. Such separated collective variables help the interpretation of molecule adsorption. All six amino acids can be adsorbed by the negatively charged surface via their backbone, irrespective of their side group. It is not surprising that Arg and Lys, whose side chains are positively charged, can also be adsorbed via their side chains.

Ions can also affect biomolecule adsorption. For example, Zheng et al. studied tripeptide (Pro–Hyp–Gly) adsorption on the rutile (110) and found that Ca^{2+} does not affect the tripeptide adsorption on the neutral surface, but leads to a strong interaction with both the negatively charged surface and the COO^- group, making the tripeptide indirectly bind with the surface and finally transform to directly bind via the COO^- group.[167] In practice, using small model molecules for studying biomolecule adsorption is a preliminary but very important attempt because a simulation containing a whole protein and solid surface is computationally costly to carry out and analyze.

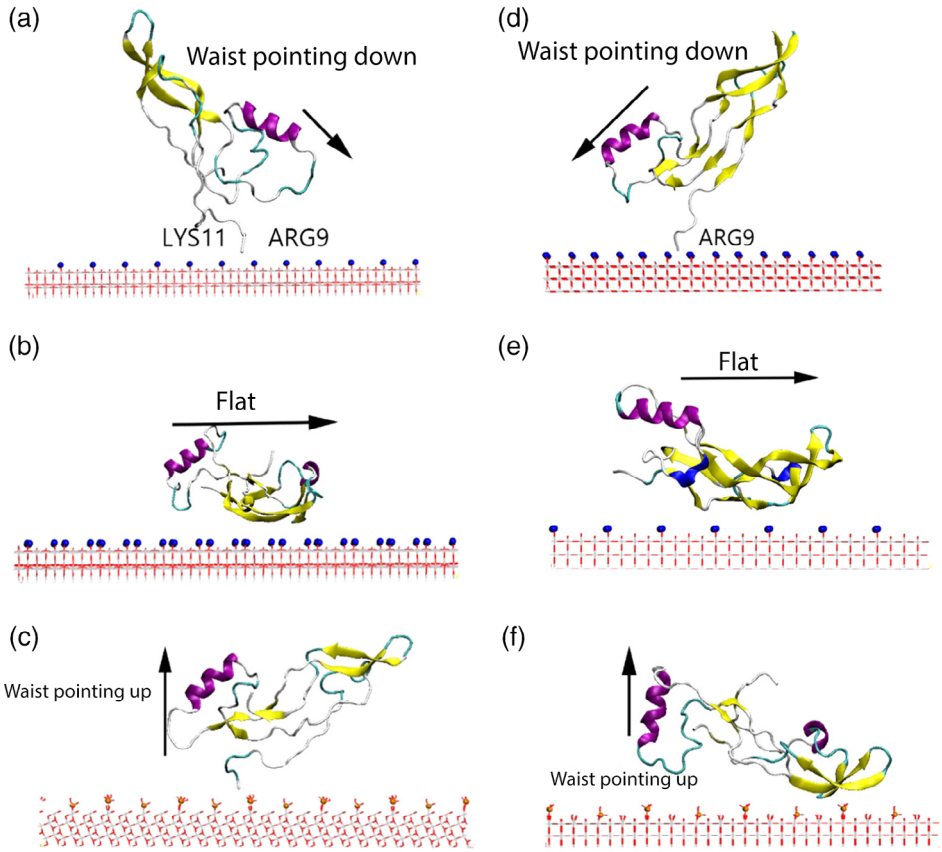

FIGURE 13 BMP-2 adsorption modes at different water/TiO_2 interfaces. Purple color highlights the wrist epitope, which shows different orientations depending on the surface terminated groups. (a,b) at the OH-terminated anatase(101) surface, the wrist epitope either points down or stays flat, (c) at the phosphite-terminated anatase(101) surface, the orientation of the BMP-2 changed and its wrist epitope points up. It also points down (d) or stays flat (e) at the OH-terminated and points up (f) at the phosphite-terminated rutile(110) surface. Reprinted with permission from Ref. 168. Copyright (2018) American Chemical Society

The next step can be to extend to simulations with biomacromolecules and a wider range of material surfaces, which can be used to predict the properties of designed biomaterials. For example, the interaction between the protein BMP-2, a growth factor for bone regeneration, and pure, OH-terminated or phosphite-modified rutile (110) and anatase (101) surfaces have been investigated, revealing two effects of phosphite-modification on promoting bone regeneration: (a) enhancing the adsorption of the BMP protein, (b) changing the orientation of BMP, making its wrist epitope point outward and bind to BMP receptor type-I on cell membranes (Figure 13(c,f)).[168] Since interactions between proteins and oxide surfaces can affect physiological functions of implanted materials and oxide surfaces can be modified by surface treatment, for example, grafting functional groups or polymers, taking advantage of MD simulations can definitely lead to better design of biomedical materials by predicting their interactions before clinical assays.

5.4 | $(SiO_2)_x{\cdot}(Al_2O_3)_y{\cdot}(MO_z)_m$

Besides silica and alumina, aluminosilicates are a significant component of the earth's crust.[169] Here, in order to avoid the complexity of the definition, we would like to discuss minerals containing silicon, aluminum, and oxygen together.

Kaolinite ($Al_2O_3 \cdot 2SiO_2 \cdot 2H_2O$), an essential material for ceramic industries, is able to adsorb cations,[170] including the nuclear waste $^{137}Cs^+$.[171] Interestingly, Zeitler et al. found that ion adsorption affects the uptake of a negatively charged crude oil model molecule at the edge kaolinite (010) surface. Although the number density of adsorbed Ca^{2+} and Na^+ are similar, Ca^{2+} enhances the uptake of oil molecules whereas Na^+ is not able to do so, providing theoretic explanation why injecting low salinity fluids can increase oil detachment from rocks to improve hydrocarbon recovery.[172]

Mica is a general name for a group of layered, sheet-like oxides of aluminum and silicon, one of which is muscovite, $KAl_2(AlSi_3)O_{10}(OH)_2$. The water/muscovite (001) interface has a flat cleavage surface and has been widely investigated by various experimental methods such as XRR and AFM. To better interpret AFM measurements of water/muscovite interfaces, Kobayashi et al. simulated AFM data by classical MD simulations.[173] After decomposing the measured force, they found that the surface first hydration layer (the water layer nearest to the solid) contributes most of the force of adhesion. Since the muscovite surface itself contains ions, an interesting question is how ions on the surface and ions in water affect each other. The muscovite (0001) lattice is hexagon-like and a K^+ sits in the center of each hexagon but under certain conditions, K^+ can be replaced by other cations. Later, they carried out MD simulations with other ions in group IA and IIA and found three binding types between cations and the surface: at the center of hexagon sites (IS1), on top of Al (IS2) or out from the surface (OS) and the formation of IS1 and IS2 is highly dependent on the charge density of the adsorbed ions.[174] The charge state of mica solid also affects cation adsorption; Jia et al. compared Na^+, K^+ and Cs^+ adsorption on mica surfaces with various charge densities and found that ion adsorption followed the sequence $Na^+ > K^+ > Cs^+$ at a low charge density surface (0.16 C/m^2 and lower) and $Cs^+ > K^+ > Na^+$ at a high one (0.24 C/m^2 and higher).[175] Mica continues to be an important model surface, for understanding ion adsorption.

6 | APPLICATIONS OF SIMULATIONS WITH OTHER OXIDE INTERFACES

6.1 | Heterogeneous catalysis

By choosing reaction coordinates carefully, the potential energy surfaces (PES) can be calculated using MD simulations and a trajectory of how reactants become products could be identified from the PES plot. The highest point on the reaction path is the transition state and its energy difference from the reactants is the reaction barrier. The protocol is successfully used to study many chemical processes, including catalysis by metals.[176]

One example we will discuss in this review is the spontaneous water dissociation at the water/CeO_2 (111) interface.[177] Farnesi Camellone et al. designed a CeO_2 surface with a Pt_6 cluster on it. They found that after a proton transfer to the CeO_2 surface, the resulting OH^- binds to a Pt site instead of the Ce site.[178] More interestingly, the dissociated water molecule can either directly dissociate at the Pt cluster, or away from the cluster; in the latter case, the resulting OH^- is quickly transferred to the Pt cluster via the Grotthuss-like proton transfer mechanism. The solvent water can help charge transfer, making an electron of OH^- move to solid Ce(IV) atom, reducing it to Ce^{3+}.[179] Such charge transfer cannot happen if no Pt cluster is on the solid surface. Similar structures, such as gold nanoparticles (AuNP) on TiO_2 surfaces are predicted to catalyze O_2 splitting for the oxidation of alcohol.[180] Muñoz-Santiburcio et al. compared the reaction mechanisms in gas phase and liquid phase to investigated how solvent water molecules enhanced the catalysis efficiency.[180] In the gas phase, the proton of the reagent, methanol, donates its hydroxyl proton to surface preadsorbed dissociated O_2 and an aliphatic hydrogen moves to the AuNP in the form of hydridic H^-. The concerted mechanism in the gas phase requires that all charge transfer happen at the same time. As a result, the substrate needs to co-adsorb to O_2 and AuNP simultaneously. However, in the liquid phase, the reaction is stepwise, decoupled in time and space. After donating the hydroxyl proton by the Grotthuss mechanism to surface dissociated O_2, the intermediate is stable and has more opportunity to adjust its configuration until an aliphatic hydrogen moves to the AuNP. In addition, in the presence of liquid water, the AuNP contains more charges that are stabilized by water solvent molecules, which can enhance the activation of surface adsorbed O_2 and the overall catalytic efficiency. This suggests that doped water/solid interfaces are promising catalysts.

However, water/solid interfaces are not always good for catalysis. One example is acetic acid ketonization on the ZrO_2 $(\bar{1}11)$ surface. By comparing the reaction paths in the gas phase and in aqueous solution, Cai et al. observed a lower reaction rate at the water/ZrO_2 interface than at the vapor/ZrO_2 interface because at high water coverage, surface sites are occupied and substrate accessibility decreased.[181] Nevertheless, water/solid interfaces are very promising systems for catalysis, especially when doped by nano-scale clusters. It can be expected that the demand for such catalysts will keep increasing and their careful design is of vital importance. As a result, AIMD simulations can be useful to predict and prescreen "future" materials.

6.2 | Prebiotic peptide formation

The polymerization of small biomolecules, such as amino acids or nucleotides, forming proteins or nucleic acids, is believed to be a fundamental process in explaining the origin of life.[75] Amino acid condensation is not favored in bulk

water but mineral surfaces, such as silica, are able to catalyze the reaction.[182] Besides silica, using $Mg_3Al(OH)_8^+$ as a model of layered double hydroxides, which were common in early earth, Erastova et al.'s MD simulations demonstrated how the mineral surface helps amino acid adsorption and alignment, as well as how wetting-drying cycles help peptide bond formation.[183]

7 | MOLECULAR DYNAMICS SIMULATIONS OF INTERFACES USING NEURAL NETWORK POTENTIALS

MD simulations are based on a mapping between any given molecular configuration and energy; this map is used to calculate forces and thus to generate a time-evolved configuration after integration of the equations of motion. The most accurate methods are those obtained from post-Hartree–Fock methods, based on quantum mechanics and a numerical solution of the Schrodinger equation. This level of accuracy is required to make reliable predictions on, for instance, molecular configurations. However, these AIMD simulations are very time-consuming even when DFT is used for solving the electronic structure problem. In classical MD simulations, complex interactions between atoms are phenomenologically captured by analytic functions of the atomic coordinates, such as bond lengths, bond angles, dihedrals and charges on atoms. This highly approximate approach is very useful because of the relatively low computational cost. However, due to the limitations of the mathematical form of force fields and the empirical process of optimally parameterizing them, the accuracy of classical MD simulations is not guaranteed and, perhaps most critically, it is difficult for classical MD to handle chemical reactions.

An alternative approach to empirical force fields, that is gaining increasing popularity, is based on neural network potentials (NNPs). This family of algorithms, traditionally employed in applications such as face recognition, self-driving cars and decision-making, can be used to calculate energies or forces for MD simulations directly from the chemical structures after proper training.[184] NNP-MD simulations have a disadvantage that the energy function cannot be easily interpreted in terms of intuitive physical concepts such as bond lengths, angles, and so on. However, its computational cost is much lower than that of AIMD. As a result, NNP-MD can also reach AIMD-level accuracy but the scale can be increased to thousands of atoms for several nanoseconds (an improvement of two orders of magnitude both in length-scale and time-scale).

The NN employed to describe the potential energy surfaces in NNP-MD use as input the Cartesian coordinates of each atom and provide, as output, the total energy and the forces acting on each atom. These are calculated by considering the local environment of each particle using either a local Cartesian frame of reference or a set of local descriptors of the molecular configuration referred to as "symmetry functions" (first proposed by Behler and Parrinello).[185,186] The latter approach makes it easier to ensure permutational symmetry of the energy function, that is, the invariance of the latter upon exchange of labels between identical particles. The total energy is then obtained through a summation over the atoms as discussed in detail in Refs. 185,186. While the NNP-MD implementation by Behler and Parrinello requires prior definition of symmetry functions, the Deep Potential techniques introduced by Weinan E's group can learn these on the fly and thus requires only Cartesian coordinates as input.[187,188] Multiple benchmarks indicate that Deep Potential can reach AIMD accuracy at a computational cost not much higher than classical simulations,[189] for example, the liquid-liquid transition of bulk water at high pressure.[190]

There are several reports of NNP-MD simulations of water/oxide interfaces.[191] One example is the interfacial proton transfer at the water/ZnO $(10\bar{1}0)$ interface.[192] NNP-MD simulations containing about 2000 atoms for nanosecond timescales were carried out and proton transfer among surface OH groups and interfacial water was observed.[192] The PMFs of proton transfer, based on the number of donated or accepted H-bonds, were calculated and it was determined that water molecules that would lose a proton preferred not to accept hydrogen bonds. However, due to the H-bond fluctuations, those water can receive one more H-bond and the barrier of proton transfer decreases. Although the fraction of interfacial water molecules accepting one H-bond is not the highest, it makes the predominant contribution to proton transfer by what is called the "presolvation" mechanism. The simulation workload is much beyond what AIMD is able to handle and classical MD simulations are not able deal with proton transfer properly, demonstrating the power of NNP-MD simulation for investigating chemical reactions in complicated environments with AIMD-level accuracy and proper statistical significance. In later works, proton transfer at both water/ZnO $(10\bar{1}0)$ and $(11\bar{2}0)$ interfaces was studied and different types of proton transfer were revealed.[193,194] At the $(10\bar{1}0)$ surface, the proton diffusion coefficient along the $(1\bar{2}10)$ direction is about 20 times higher than that along the (0001) direction, indicating that proton transfer is "pseudo-one-dimensional"; however, at the $(11\bar{2}0)$ surface, proton transfer is two dimensional, along both the $(1\bar{1}00)$

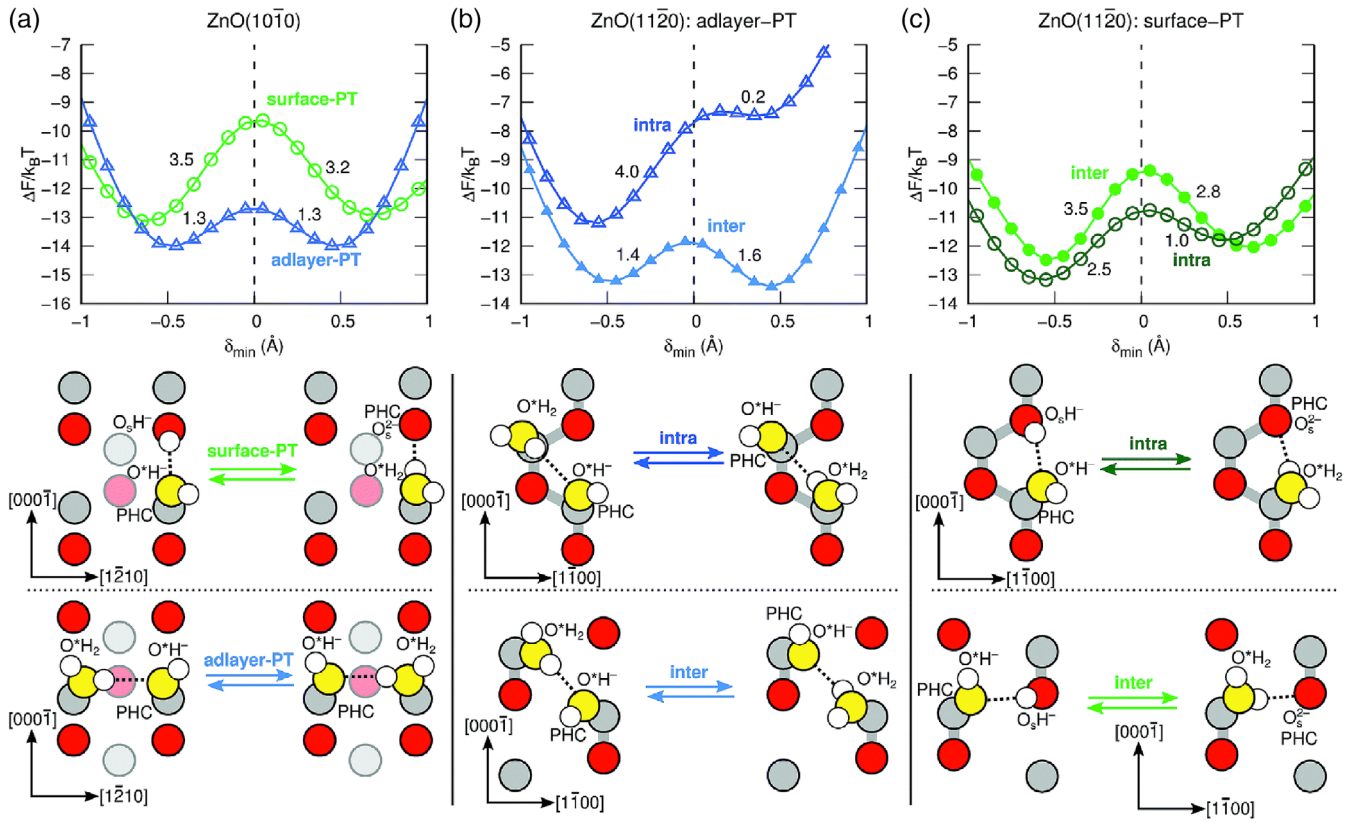

FIGURE 14 Free energy profile of proton transfer from NNP-MD simulations at the (a) ZnO (10$\bar{1}$0) interface and (b,c) ZnO (11$\bar{2}$0) interface. For the ZnO (10$\bar{1}$0) interface, proton transfer along the (0001) direction has a high barrier (3.5 k_BT, green in (a)), but that along the (1$\bar{2}$10) is more accessible. For the ZnO (11$\bar{2}$0) interface, proton transfer is along both two directions. Reprinted from Ref. 193—Published by The Royal Society of Chemistry

and the (0001) directions (Figure 14). The NNP-MD simulations are also used to study the vibrational spectra of the water/ZnO (10$\bar{1}$0) interface, finding that the frequency of water species within 4 Å of the surface were perturbed. They decompose the total OH vibrational spectra into contributions for each water species though their signals basically overlap together. This work shows that NNP-MD simulations can not only reproduce the structure and energy as AIMD, but it can also provide reliable dynamics. Now, NNP-MD has been implemented in LAMMPS.[195]

8 | THE FUTURE AND CHALLENGE OF THIS FIELD

As pointed out in previous sections, the applications of MD simulations have grown rapidly in recent years thanks to increased computational resources. However, MD simulations are not panaceas to investigate all chemical processes near water/oxide interfaces. We list several limitations and challenges of current MD simulations and expect that breakthroughs could be made to increase the impact of this field.

Perfect, defect absent solid surfaces were used in most simulations as a model of "real" surfaces in experimental conditions. Such a simplification could be used for stable surfaces but in the real world, besides intrinsic defects of mineral crystals, dissolution and precipitation keep reshaping the interfaces. However, how such processes affect local water structure is unknown.

Second, when the ion concentration is low, the thickness of interfacial region could be as long as 10–100 nm, making simulations of the interfacial region at all-atomic level slow and ineffective. It will be a good practice to perform multiscale modeling with a simplified diffuse layer to reduce simulation cost and keep the interfacial region complete.

MD simulations of aqueous/oxide interfaces often seek comparisons with experimental data. The vibrational spectra of water are a common target but contain features that are challenging to calculate; namely the bend + liberation combination band which contributes a broad feature near 2100 cm^{-1} and the Fermi resonance of the bend overtone with

the symmetric stretch.[198] In addition, other modes such as the bend +stretch combination band have the advantage of eliminating complications of the Fermi resonance and can allow for H_2O and surface hydroxyls modes to be distinguished.[199] Accurate calculations of these important experimental observables are key to successful microscopic interpretation. Progress in this area could have a major impact on our understanding of aqueous interfaces and bulk water environments.

Other limitations in MD simulations, such as the accuracy of force fields, the limited time/length scales of simulations and the neglect of nuclear quantum effects are not inevitable in MD simulations of water/oxide interfaces. Besides those theoretical concerns, we expect that more software tools could be developed to accelerate the preparation and analysis of simulation results, such as web-based CHARMM-GUI,[196] which supports modeling mineral surfaces. In addition, new technologies such as virtual reality could help the visualization of MD simulations.[197]

9 | CONCLUSION

We have reviewed computational MD simulations of water/oxide interfaces, with a focus on chemical processes, such as water or small molecule adsorption, pK_a calculation near interfaces and heterogeneous catalysis. The behavior of interfacial water is quite different from that in the bulk and more sophisticated descriptions than approximations based-on mean-field levels, such as EDL theory, are required. Solutes, such as ions or biomolecules, can adsorb onto the surface and further affect interfacial water structures. Using AIMD, the pK_a of surface OH groups, the pK_a of solutes near interfaces and how solutes affect surface pK_a, can be investigated. From MD simulations, vibrational spectra, such as widely reported vSFG, can be calculated and compared with experimental measures. Chemical reactions at interfaces, such as catalytic water splitting at water/TiO_2 interfaces, can also be studied by MD simulations which reveal the estimated free energy profile and the catalytic mechanism. The microscopic insight provided by computational studies advances our understanding of the chemistry and physics at water/solid interfaces and complements experimental characterizations. Lastly, to overcome current limitations in classical MD and AIMD simulations, NNP-MD simulations can enlarge the scale of AIMD-like simulations to the level of classical simulations without the loss of accuracy at a reasonable cost, which could be a promising method for MD simulations in the future.

ACKNOWLEDGMENTS

This work was supported as part of the Center for Complex Materials from First Principles (CCM), an Energy Frontier Research Center funded by the U.S. Department of Energy, Office of Science, Basic Energy Sciences under Award #DE-SC0012575. E.B. acknowledges and thanks the National Science Foundation for its support (NSF Grant MRI 1828421). This work was funded by the National Institutes of Health (R01GM093290, R01GM131048, S10OD020095 to V.C.), and the National Science Foundation grant IOS-1934848 to V.C. R.W. thanks Temple University for the support of a Presidential Fellowship.

CONFLICT OF INTEREST

The authors have declared no conflicts of interest for this article.

AUTHOR CONTRIBUTIONS

Ruiyu Wang: Conceptualization; writing-original draft; writing-review & editing. **Michael Klein:** Conceptualization; writing-review & editing. **Vincenzo Carnevale:** Conceptualization; writing-review & editing. **Eric Borguet:** Conceptualization; writing-review & editing.

DATA AVAILABILITY STATEMENT

Data sharing is not applicable to this article as no new data were created or analyzed in this study.

ORCID

Ruiyu Wang https://orcid.org/0000-0003-1608-140X
Vincenzo Carnevale https://orcid.org/0000-0002-1918-8280
Eric Borguet https://orcid.org/0000-0003-0593-952X

RELATED WIREs ARTICLES

Organic-inorganic interface simulation for new material discoveries
Advanced models for water simulations.

REFERENCES

1. Björneholm O, Hansen MH, Hodgson A, Liu L-M, Limmer DT, Michaelides A, et al. Water at interfaces. *Chem Rev*. 2016;*116*(13):7698–7726.
2. Taylor CD, Neurock M. Theoretical insights into the structure and reactivity of the aqueous/metal Interface. *Curr Opin Solid State Mater Sci*. 2005;*9*(1):49–65.
3. Carrasco J, Hodgson A, Michaelides A. A molecular perspective of water at metal interfaces. *Nat Mater*. 2012;*11*:667.
4. Felix Sedlmeier JJ, Sendner C, Bocquet L, Netz RR, Horinek D. Water at polar and nonpolar solid walls (review). *Biointerphases*. 2008;*3*(3):FC23–39.
5. Rimola A, Sodupe M, Ugliengo P. Aluminosilicate surfaces as promoters for peptide bond formation: an assessment of Bernal's hypothesis by ab initio methods. *J Am Chem Soc*. 2007;*129*(26):8333–44.
6. Rimola A, Sodupe M, Ugliengo P. Role of mineral surfaces in prebiotic chemical evolution in silico quantum mechanical studies. *Life*. 2019;*9*(1):10.
7. Sakong S, Forster-Tonigold K, Groß A. The structure of water at a Pt(111) electrode and the potential of zero charge studied from first principles. *J Chem Phys*. 2016;*144*(19):194701.
8. McKendry IG, Thenuwara AC, Shumlas SL, Peng H, Aulin YV, Chinnam PR, et al. Systematic doping of cobalt into layered manganese oxide sheets substantially enhances water oxidation catalysis. *Inorg Chem*. 2018;*57*(2):557–64.
9. Attanayake NH, Thenuwara AC, Patra A, Aulin YV, Tran TM, Chakraborty H, et al. Effect of intercalated metals on the electrocatalytic activity of 1T-MoS_2 for the hydrogen evolution reaction. *ACS Energy Lett*. 2018;*3*(1):7–13.
10. Sakong S, Groß A. The electric double layer at metal-water interfaces revisited based on a charge polarization scheme. *J Chem Phys*. 2018;*149*(8):084705.
11. Helmholtz H. Studien über electrische grenzschichten. *Ann Phys*. 1879;*243*(7):337–82.
12. Gouy-Chapman SG. *Theory. Encyclopedia of geochemistry: a comprehensive reference source on the chemistry of the earth*. Cham: Springer International Publishing; 2018.p. 623–8.
13. Chapman DL, Li. A contribution to the theory of electrocapillarity. *London Edinburgh Dublin Philos Mag J Sci*. 1913;*25*(148):475–81.
14. Gouy M. Sur la constitution de la charge électrique à la surface d'un électrolyte. *J Phys Theor Appl*. 1910;*9*(1):457–68.
15. Backus E, Schaefer J, Bonn M. The mineral/water interface probed with nonlinear optical spectroscopy. *Angew Chem Int Ed*. 2020.
16. Stern O. Zur theorie der elektrolytischen doppelschicht. *Z Elektrochem Angew Phys Chem*. 1924;*30*:508–16.
17. Elimelech M, Gregory J, Jia X, Williams RA. Chapter 2 - electrical properties of interfaces. *Particle deposition & aggregation*. Woburn: Butterworth-Heinemann; 1995. p. 9–32.
18. Dewan S, Carnevale V, Bankura A, Eftekhari-Bafrooei A, Fiorin G, Klein ML, et al. Structure of water at charged interfaces: a molecular dynamics study. *Langmuir*. 2014;*30*(27):8056–65.
19. Fenter P, Sturchio NC. Mineral–water interfacial structures revealed by synchrotron X-ray scattering. *Prog Surf Sci*. 2004;*77*(5):171–258.
20. Santos S, Verdaguer A. Imaging water thin films in ambient conditions using atomic force microscopy. *Materials*. 2016;*9*(3):182.
21. Mu R, Zhao Z-J, Dohnálek Z, Gong J. Structural motifs of water on metal oxide surfaces. *Chem Soc Rev*. 2017;*46*(7):1785–806.
22. Covert PA, Hore DK. Geochemical insight from nonlinear optical studies of mineral–water interfaces. *Annu Rev Phys Chem*. 2016;*67*(1):233–57.
23. Takagi Y, Uruga T, Tada M, Iwasawa Y, Yokoyama T. Ambient pressure hard X-ray photoelectron spectroscopy for functional material systems as fuel cells under working conditions. *Acc Chem Res*. 2018;*51*(3):719–27.
24. Li H, Yan T, Fichthorn KA. Influence of gravity on the sliding angle of water drops on nanopillared superhydrophobic surfaces. *Langmuir*. 2020;*36*(33):9916–25.
25. Lamour G, Hamraoui A, Buvailo A, Xing Y, Keuleyan S, Prakash V, et al. Contact angle measurements using a simplified experimental setup. *J Chem Educ*. 2010;*87*(12):1403–7.
26. Harmon KJ, Chen Y, Bylaska EJ, Catalano JG, Bedzyk MJ, Weare JH, et al. Insights on the alumina–water interface structure by direct comparison of density functional simulations with X-ray reflectivity. *J Phys Chem C*. 2018;*122*(47):26934–44.
27. Catalano JG. Weak interfacial water ordering on isostructural hematite and corundum (0 0 1) surfaces. *Geochim Cosmochim Acta*. 2011;*75*:2062–71.
28. Catalano JG. Relaxations and interfacial water ordering at the corundum (110) surface. *J Phys Chem C*. 2010;*114*(14):6624–30.
29. Catalano JG, Park C, Zhang Z, Fenter P. Termination and water adsorption at the α- Al_2O_3(012)−aqueous solution interface. *Langmuir*. 2006;*22*(10):4668–73.
30. Tuladhar A, Piontek SM, Frazer L, Borguet E. Effect of halide anions on the structure and dynamics of water next to an alumina (0001) surface. *J Phys Chem C*. 2018;*122*(24):12819–30.
31. Tuladhar A, Piontek SM, Borguet E. Insights on interfacial structure, dynamics, and proton transfer from ultrafast vibrational sum frequency generation spectroscopy of the alumina(0001)/water Interface. *J Phys Chem C*. 2017;*121*(9):5168–77.

32. Zhang L, Tian C, Waychunas GA, Shen YR. Structures and charging of α-alumina (0001)/water interfaces studied by sum-frequency vibrational spectroscopy. *J Am Chem Soc*. 2008;*130*(24): 7686–94.
33. Tuladhar A, Dewan S, Kubicki JD, Borguet E. Spectroscopy and ultrafast vibrational dynamics of strongly hydrogen bonded OH species at the α-Al_2O_3 (11$\bar{2}$0)/H_2O interface. *J Phys Chem C*. 2016;*120*(29):16153–61.
34. Eftekhari-Bafrooei A, Borguet E. Effect of surface charge on the vibrational dynamics of interfacial water. *J Am Chem Soc*. 2009;*131*(34):12034–35.
35. Eftekhari-Bafrooei A, Borguet E. Effect of hydrogen-bond strength on the vibrational relaxation of interfacial water. *J Am Chem Soc*. 2010;*132*(11):3756–61.
36. Eftekhari-Bafrooei A, Borguet E. Effect of electric fields on the ultrafast vibrational relaxation of water at a charged solid–liquid interface as probed by vibrational sum frequency generation. *J Phys Chem Lett*. 2011;*2*(12):1353–8.
37. Humphrey W, Dalke A, Schulten K. VMD: visual molecular dynamics. *J Mol Graph*. 1996;*14*(1):33–8.
38. McGibbon RT, Beauchamp KA, Harrigan MP, Klein C, Swails JM, Hernández CX, et al. MDTraj: a modern open library for the analysis of molecular dynamics trajectories. *Biophys J*. 2015;*109*(8):1528–32.
39. Richard J. Gowers ML, Jonathan Barnoud, Tyler J. E. Reddy, Manuel N. Melo, Sean L. Seyler, Jan Domański, David L. Dotson, Sébastien Buchoux, Ian M. Kenney and Oliver Beckstein. MD analysis: a python package for the rapid analysis of molecular dynamics simulations. In Proceedings of the 15th Python in Science Conference. 2016. p. 98–105.
40. Michaud-Agrawal N, Denning EJ, Woolf TB, Beckstein O. MDAnalysis: a toolkit for the analysis of molecular dynamics simulations. *J Comput Chem*. 2011;*32*(10):2319–27.
41. Striolo A. From interfacial water to macroscopic observables: a review. *Adsorpt Sci Technol*. 2011;*29*(3):211–58.
42. Striolo A, Michaelides A, Joly L. The carbon-water interface: modeling challenges and opportunities for the water-energy nexus. *Annu Rev Chem Biomol Eng*. 2016;*7*(1):533–56.
43. YazdanYar A, Aschauer U, Bowen P. Interaction of biologically relevant ions and organic molecules with titanium oxide (rutile) surfaces: a review on molecular dynamics studies. *Colloids Surf B Biointerfaces*. 2018;*161*:563–77.
44. Verlet L. Computer "experiments" on classical fluids. I. Thermodynamical properties of Lennard-Jones molecules. *Phys Rev*. 1967;*159*(1):98–103.
45. Frenkel D, Smit B. *Understanding molecular simulation: from algorithms to applications*. Amsterdam, Netherlands: Elsevier; 2001.
46. Allen MP, Tildesley DJ. *Computer simulation of liquids*. Oxford, England: Oxford University Press; 2017.
47. Phillips JC, Braun R, Wang W, Gumbart J, Tajkhorshid E, Villa E, et al. Scalable molecular dynamics with NAMD. *J Comput Chem*. 2005;*26*(16):1781–802.
48. Xue M, Guo W. Water models for interfacial water simulations. *Sci China Tech Sci*. 2019;*62*(5):729–735.
49. Demerdash O, Wang LP, Head-Gordon T. Advanced models for water simulations. *WIREs Comput Mol Sci*. 2018;*8*(1):e1355.
50. Remsing RC, Duignan TT, Baer MD, Schenter GK, Mundy CJ, Weeks JD. Water lone pair delocalization in classical and quantum descriptions of the hydration of model ions. *J Phys Chem B*. 2018;*122*(13):3519–27.
51. van Duin ACT, Dasgupta S, Lorant F, Goddard WA. Reaxff: a reactive force field for hydrocarbons. *J Phys Chem A*. 2001;*105*(41):9396–409.
52. Baskes MI. Modified embedded-atom potentials for cubic materials and impurities. *Phys Rev B*. 1992;*46*(5):2727–42.
53. Shan T-R, Devine BD, Kemper TW, Sinnott SB, Phillpot SR. Charge-optimized many-body potential for the hafnium/hafnium oxide system. *Phys Rev B*. 2010;*81*(12):125328.
54. Raju M, Kim S-Y, van Duin ACT, Fichthorn KA. ReaxFF reactive force field study of the dissociation of water on titania surfaces. *J Phys Chem C*. 2013;*117*(20):10558–72.
55. Senftle TP, Hong S, Islam MM, Kylasa SB, Zheng Y, Shin YK, et al. The ReaxFF reactive force-field: development, applications and future directions. *npj Comput Mater*. 2016;*2*:15011.
56. Car R, Parrinello M. Unified approach for molecular dynamics and density-functional theory. *Phys Rev Lett*. 1985;*55*(22):2471–4.
57. Iftimie R, Minary P, Tuckerman ME. Ab initio molecular dynamics: concepts, recent developments, and future trends. *Proc Natl Acad Sci U S A*. 2005;*102*(19):6654–9.
58. Alder BJ, Wainwright TE. Phase transition for a hard sphere system. *J Chem Phys*. 1957;*27*(5):1208–9.
59. Rahman A. Correlations in the motion of atoms in liquid argon. *Phys Rev*. 1964;*136*(2A):A405–A11.
60. Rahman A, Stillinger FH. Molecular dynamics study of liquid water. *J Chem Phys*. 1971;*55*(7):3336–59.
61. Watanabe H, Suzuki M, Ito N. Huge-scale molecular dynamics simulation of multibubble nuclei. *Comput Phys Commun*. 2013;*184*(12):2775–84.
62. Shaw DE, Dror RO, Salmon JK, Grossman J, Mackenzie KM, Bank JA, et al. Millisecond-scale molecular dynamics simulations on anton. In Proceedings of the conference on high performance computing networking, storage and analysis; 2009.
63. Baer MD, Kuo IFW, Tobias DJ, Mundy CJ. Toward a unified picture of the water self-ions at the air–water interface: a density functional theory perspective. *J Phys Chem B*. 2014;*118*(28):8364–72.
64. Cheng J, Liu X, VandeVondele J, Sprik M. Reductive hydrogenation of the aqueous rutile TiO_2(110) surface. *Electrochim Acta*. 2015;*179*:658–67.
65. Hass KC, Schneider WF, Curioni A, Andreoni W. The chemistry of water on alumina surfaces: reaction dynamics from first principles. *Science*. 1998;*282*(5387):265–8.

66. Hass KC, Schneider WF, Curioni A, Andreoni W. First-principles molecular dynamics simulations of H_2O on α-Al_2O_3 (0001). *J Phys Chem B*. 2000;*104*(23):5527–40.
67. Hoover WG. Canonical dynamics: equilibrium phase-space distributions. *Phys Rev A*. 1985;*31*(3):1695–7.
68. Nosé S. A unified formulation of the constant temperature molecular dynamics methods. *J Chem Phys*. 1984;*81*(1):511–9.
69. Nosé S. A molecular dynamics method for simulations in the canonical ensemble. *Mol Phys*. 1984;*52*(2):255–68.
70. Martyna GJ, Tuckerman ME, Tobias DJ, Klein ML. Explicit reversible integrators for extended systems dynamics. *Mol Phys*. 1996;*87*(5):1117–57.
71. Rimola A, Costa D, Sodupe M, Lambert JF, Ugliengo P. Silica surface features and their role in the adsorption of biomolecules: computational modeling and experiments. *Chem Rev*. 2013;*113*(6):4216–313.
72. Frank ES, Fan H, Shrestha M, Riahi S, Tobias DJ, Grassian VH. Impact of adsorbed water on the interaction of limonene with hydroxylated SiO_2: implications of π-hydrogen bonding for surfaces in humid environments. *J Phys Chem A*. 2020;*124*(50):10592–9.
73. Jia J, Liang Y, Tsuji T, Miranda CR, Masuda Y, Matsuoka T. Ab initio molecular dynamics study of carbonation and hydrolysis reactions on cleaved quartz (001) surface. *J Phys Chem C*. 2019;*123*(8):4938–48.
74. Sun EWH, Bourg IC. Molecular dynamics simulations of mineral surface wettability by water versus CO_2: thin films, contact angles, and capillary pressure in a silica nanopore. *J Phys Chem C*. 2020;*124*(46):25382–95.
75. Rimola A, Fabbiani M, Sodupe M, Ugliengo P, Martra G. How does silica catalyze the amide bond formation under dry conditions? Role of specific surface silanol pairs. *ACS Catal*. 2018;*8*(5):4558–68.
76. Isaienko O, Borguet E. Hydrophobicity of hydroxylated amorphous fused silica surfaces. *Langmuir*. 2013;*29*(25):7885–95.
77. Anderson RS, Anderson SP. *Geomorphology: the mechanics and chemistry of landscapes*. Cambridge: Cambridge University Press; 2010.
78. Ong S, Zhao X, Eisenthal KB. Polarization of water molecules at a charged interface: second harmonic studies of the silica/water interface. *Chem Phys Lett*. 1992;*191*(3):327–35.
79. Gaigeot M-P, Sprik M, Sulpizi M. Oxide/water interfaces: how the surface chemistry modifies interfacial water properties. *J Phys Condens Matter*. 2012;*24*(12):124106.
80. Hocine S, Hartkamp R, Siboulet B, Duvail M, Coasne B, Turq P, et al. How ion condensation occurs at a charged surface: a molecular dynamics investigation of the Stern layer for water–silica interfaces. *J Phys Chem C*. 2016;*120*(2):963–73.
81. Bouhadja M, Skelton AA. Dynamical properties of water and ions at the quartz (101)–water interface at a range of solution conditions: a classical molecular dynamics study. *J Phys Chem C*. 2018;*122*(3):1535–46.
82. Kroutil O, Chval Z, Skelton AA, Předota M. Computer simulations of quartz (101)–water Interface over a range of pH values. *J Phys Chem C*. 2015;*119*(17):9274–86.
83. Brkljača Z, Namjesnik D, Lützenkirchen J, Předota M, Preočanin T. Quartz/aqueous electrolyte solution interface: molecular dynamic simulation and interfacial potential measurements. *J Phys Chem C*. 2018;*122*(42):24025–36.
84. Quezada GR, Rozas RE, Toledo PG. Molecular dynamics simulations of quartz (101)–water and corundum (001)–water interfaces: effect of surface charge and ions on cation adsorption, water orientation, and surface charge reversal. *J Phys Chem C*. 2017;*121*(45):25271–82.
85. Pfeiffer-Laplaud M, Gaigeot MP. Adsorption of singly charged ions at the hydroxylated (0001) α-quartz/water Interface. *J Phys Chem C*. 2016;*120*(9):4866–80.
86. DelloStritto MJ, Kubicki JD, Sofo JO. Effect of ions on H-bond structure and dynamics at the quartz(101)–water interface. *Langmuir*. 2016;*32*(44):11353–65.
87. Leung K, Criscenti LJ, Knight AW, Ilgen AG, Ho TA, Greathouse JA. Concerted metal cation desorption and proton transfer on deprotonated silica surfaces. *J Phys Chem Lett*. 2018;*9*(18):5379–85.
88. Pfeiffer-Laplaud M, Gaigeot MP. Electrolytes at the hydroxylated (0001) α-quartz/water interface: location and structural effects on interfacial silanols by DFT-based MD. *J Phys Chem C*. 2016;*120*(26):14034–47.
89. Chen S-H, Singer SJ. Molecular dynamics study of the electric double layer and nonlinear spectroscopy at the amorphous silica–water interface. *J Phys Chem B*. 2019;*123*(29):6364–84.
90. Kolman K, Abbas Z. Molecular dynamics exploration for the adsorption of benzoic acid derivatives on charged silica surfaces. *Colloids Surf Physicochem Eng Aspects*. 2019;*578*:123635.
91. Döpke MF, Lützenkirchen J, Moultos OA, Siboulet B, Dufrêche J-F, Padding JT, et al. Preferential adsorption in mixed electrolytes confined by charged amorphous silica. *J Phys Chem C*. 2019;*123*(27):16711–20.
92. Buch V, Milet A, Vácha R, Jungwirth P, Devlin JP. Water surface is acidic. *Proc Natl Acad Sci U S A*. 2007;*104*(18):7342–7.
93. Tse Y-LS, Chen C, Lindberg GE, Kumar R, Voth GA. Propensity of hydrated excess protons and hydroxide anions for the air–water interface. *J Am Chem Soc*. 2015;*137*(39):12610–6.
94. Pezzotti S, Gaigeot M-P. Spectroscopic BIL-SFG invariance hides the chaotropic effect of protons at the air-water interface. *Atmos*. 2018;*9*(10):396.
95. Giberti F, Hassanali AA. The excess proton at the air-water Interface: the role of instantaneous liquid interfaces. *J Chem Phys*. 2017;*146*(24):244703.
96. Mundy CJ, Kuo IFW, Tuckerman ME, Lee H-S, Tobias DJ. Hydroxide anion at the air–water interface. *Chem Phys Lett*. 2009;*481*(1):2–8.
97. Beattie JK, Djerdjev AM, Warr GG. The surface of neat water is basic. *Faraday Discuss*. 2009;*141*:31–9.

98. Mishra H, Enami S, Nielsen RJ, Stewart LA, Hoffmann MR, Goddard WA, et al. Brønsted basicity of the air–water Interface. *Proc Natl Acad Sci U S A*. 2012;*2012*:09307.
99. Sulpizi M, Gaigeot M-P, Sprik M. The silica–water Interface: how the Silanols determine the surface acidity and modulate the water properties. *J Chem Theory Comput*. 2012;*8*(3):1037–47.
100. Pfeiffer-Laplaud M, Gaigeot MP, Sulpizi M. pK_a at quartz/electrolyte interfaces. *J Phys Chem Lett*. 2016;*7*(16):3229–34.
101. Pfeiffer-Laplaud M, Costa D, Tielens F, Gaigeot MP, Sulpizi M. Bimodal acidity at the amorphous silica/water Interface. *J Phys Chem C*. 2015;*119*(49):27354–62.
102. Parashar S, Lesnicki D, Sulpizi M. Increased acid dissociation at the quartz/water Interface. *J Phys Chem Lett*. 2018;*9*(9):2186–9.
103. Sulpizi M, Sprik M. Acidity constants from vertical energy gaps: density functional theory based molecular dynamics implementation. *Phys Chem Chem Phys*. 2008;*10*(34):5238–49.
104. Joutsuka T, Hirano T, Sprik M, Morita A. Effects of third-order susceptibility in sum frequency generation spectra: a molecular dynamics study in liquid water. *Phys Chem Chem Phys*. 2018;*20*(5):3040–53.
105. Morita A, Ishiyama T. Recent progress in theoretical analysis of vibrational sum frequency generation spectroscopy. *Phys Chem Chem Phys*. 2008;*10*(38):5801–16.
106. Pezzotti S, Galimberti DR, Shen YR, Gaigeot M-P. Structural definition of the BIL and DL: a new universal methodology to rationalize non-linear $^{(2)}(\omega)$ SFG signals at charged interfaces, including $\chi^{(3)}(\omega)$ contributions. *Phys Chem Chem Phys*. 2018;*20*(7):5190–9.
107. Pezzotti S, Galimberti DR, Gaigeot M-P. Deconvolution of BIL-SFG and DL-SFG spectroscopic signals reveals order/disorder of water at the elusive aqueous silica interface. *Phys Chem Chem Phys*. 2019;*21*(40):22188–202.
108. Ohto T, Dodia M, Xu J, Imoto S, Tang F, Zysk F, et al. Accessing the accuracy of density functional theory through structure and dynamics of the water–air interface. *J Phys Chem Lett*. 2019;*10*(17):4914–9.
109. Smit WJ, Tang F, Sánchez MA, Backus EHG, Xu L, Hasegawa T, et al. Excess hydrogen bond at the ice-vapor interface around 200 K. *Phys Rev Lett*. 2017;*119*(13):133003.
110. Reddy SK, Thiraux R, Wellen Rudd BA, Lin L, Adel T, Joutsuka T, et al. Bulk contributions modulate the sum-frequency generation spectra of water on model sea-spray aerosols. *Chem*. 2018;*4*(7):1629–44.
111. Seki T, Sun S, Zhong K, Yu C-C, Machel K, Dreier LB, et al. Unveiling heterogeneity of interfacial water through the water bending mode. *J Phys Chem Lett*. 2019;*10*(21):6936–41.
112. Wen Y-C, Zha S, Liu X, Yang S, Guo P, Shi G, et al. Unveiling microscopic structures of charged water interfaces by surface-specific vibrational spectroscopy. *Phys Rev Lett*. 2016;*116*(1):016101.
113. Dewan S, Yeganeh MS, Borguet E. Experimental correlation between interfacial water structure and mineral reactivity. *J Phys Chem Lett*. 2013;*4*(11):1977–82.
114. Tuladhar A, Dewan S, Pezzotti S, Brigiano FS, Creazzo F, Gaigeot MP, Borguet E. Ions tune interfacial water structure and modulate hydrophobic interactions at silica surfaces. *J Am Chem Soc*. 2020;*142*(15):6991–7000.
115. Campen RK, Pymer AK, Nihonyanagi S, Borguet E. Linking surface potential and deprotonation in nanoporous silica: second harmonic generation and acid/base titration. *J Phys Chem C*. 2010;*114*(43):18465–73.
116. Fertani-Gmati M, Jemal M. Thermochemistry and kinetics of silica dissolution in NaOH aqueous solution. *Thermochim Acta*. 2011;*513*(1):43–8.
117. Du J, Rimsza JM. Atomistic computer simulations of water interactions and dissolution of inorganic glasses. *npj Mater Degrad*. 2017;*1*(1):16.
118. Rimsza JM, Yeon J, van Duin ACT, Du J. Water interactions with nanoporous silica: comparison of ReaxFF and ab initio based molecular dynamics simulations. *J Phys Chem C*. 2016;*120*(43):24803–16.
119. Rimsza JM, Du J. Interfacial structure and evolution of the water–silica gel system by reactive force-field-based molecular dynamics simulations. *J Phys Chem C*. 2017;*121*(21):11534–43.
120. Santos PS, Santos HS, Toledo SP. Standard transition aluminas electron microscopy studies. *Mater Res*. 2000;*3*:104–14.
121. Feng JT, He YF, Liu YN, Du YY, Li DQ. Supported catalysts based on layered double hydroxides for catalytic oxidation and hydrogenation: general functionality and promising application prospects. *Chem Soc Rev*. 2015;*44*(15):5291–319.
122. Réocreux R, Jiang T, Iannuzzi M, Michel C, Sautet P. Structuration and dynamics of interfacial liquid water at hydrated γ-alumina determined by ab initio molecular simulations: implications for nanoparticle stability. *ACS Appl Nano Mater*. 2018;*1*(1):191–9.
123. Argyris D, Ho T, Cole DR, Striolo A. Molecular dynamics studies of interfacial water at the alumina surface. *J Phys Chem C*. 2011;*115*(5):2038–46.
124. Ridley MK, Tunega D. Insights on the structural and dynamic properties of corundum–water interfaces from first-principle molecular dynamics. *J Phys Chem C*. 2021;*125*(1):295–309.
125. Wang R, DelloStritto M, Remsing RC, Carnevale V, Klein ML, Borguet E. Sodium halide adsorption and water structure at the α-alumina(0001)/water interface. *J Phys Chem C*. 2019;*123*(25):15618–28.
126. Cygan RT, Liang J-J, Kalinichev AG. Molecular models of hydroxide, oxyhydroxide, and clay phases and the development of a general force field. *J Phys Chem B*. 2004;*108*(4):1255–66.
127. Pouvreau M, Greathouse JA, Cygan RT, Kalinichev AG. Structure of hydrated kaolinite edge surfaces: DFT results and further development of the ClayFF classical force field with metal–O–H angle bending terms. *J Phys Chem C*. 2019;*123*(18):11628–38.
128. DelloStritto M, Sofo J. Bond polarizability model for sum frequency generation at the $Al_2O_3(0001)$–H_2O interface. *J Phys Chem A*. 2017;*121*(16):3045–55.

129. Braunschweig B, Eissner S, Daum W. Molecular structure of a mineral/water interface: effects of surface nanoroughness of α-Al_2O_3(0001). *J Phys Chem C*. 2008;*112*(6):1751–4.
130. DelloStritto M, Piontek SM, Klein ML, Borguet E. Relating interfacial order to sum frequency generation with ab initio simulations of the aqueous Al_2O_3(0001) and (112$\bar{c}$0) interfaces. *J Phys Chem C*. 2018;*122*(37):21284–94.
131. DelloStritto MJ, Piontek SM, Klein ML, Borguet E. Effect of functional and electron correlation on the structure and spectroscopy of the Al_2O_3(001)–H_2O Interface. *J Phys Chem Lett*. 2019;*10*(9):2031–6.
132. Sun J, Ruzsinszky A, Perdew JP. Strongly constrained and appropriately normed Semilocal density functional. *Phys Rev Lett*. 2015;*115*(3):036402.
133. Chen M, Ko HY, Remsing RC, Calegari Andrade MF, Santra B, Sun Z, et al. Ab initio theory and modeling of water. *Proc Natl Acad Sci U S A*. 2017;*114*(41):10846–51.
134. Zheng L, Chen M, Sun Z, Ko H-Y, Santra B, Dhuvad P, et al. Structural, electronic, and dynamical properties of liquid water by ab initio molecular dynamics based on SCAN functional within the canonical ensemble. *J Chem Phys*. 2018;*148*(16):164505.
135. Xu J, Chen M, Zhang C, Wu X. First-principles study of the infrared Spectrum in liquid water from a systematically improved description of H-bond network. *Phys Rev B*. 2019;*99*(20):205123.
136. Wang R, Carnevale V, Klein ML, Borguet E. First-principles calculation of water pK_a using the newly developed SCAN functional. *J Phys Chem Lett*. 2020;*11*:54–9.
137. DelloStritto M, Xu J, Wu X, Klein ML. Aqueous solvation of the chloride ion revisited with density functional theory: impact of correlation and exchange approximations. *Phys Chem Chem Phys*. 2020;*22*(19):10666–75.
138. Melani G, Nagata Y, Wirth J, Saalfrank P. Vibrational spectroscopy of hydroxylated α-Al_2O_3(0001) surfaces with and without water: an ab initio molecular dynamics study. *J Chem Phys*. 2018;*149*(1):014707.
139. Harmon KJ, Letchworth-Weaver K, Gaiduk AP, Giberti F, Gygi F, Chan MKY, et al. Validating first-principles molecular dynamics calculations of oxide/water interfaces with X-ray reflectivity data. *Phys Rev Mater*. 2020;*4*(11):113805.
140. Liu X, Cheng J, Sprik M, Lu X, Wang R. Understanding surface acidity of gibbsite with first principles molecular dynamics simulations. *Geochim Cosmochim Acta*. 2013;*120*:487–95.
141. Contescu C, Jagiello J, Schwarz JA. Heterogeneity of proton binding sites at the oxide/solution Interface. *Langmuir*. 1993;*9*(7):1754–65.
142. Gittus OR, von Rudorff GF, Rosso KM, Blumberger J. Acidity constants of the hematite–liquid water interface from ab initio molecular dynamics. *J Phys Chem Lett*. 2018;*9*(18):5574–82.
143. Jia M, Zhang C, Cox SJ, Sprik M, Cheng J. Computing surface acidity constants of proton hopping groups from density functional theory-based molecular dynamics: application to the SnO_2(110)/H_2O interface. *J Chem Theory Comput*. 2020;*16*(10):6520–7.
144. Diebold U. The surface science of titanium dioxide. *Surf Sci Rep*. 2003;*48*(5):53–229.
145. Rousseau R, Glezakou VA, Selloni A. Theoretical insights into the surface physics and chemistry of redox-active oxides. *Nature Reviews Materials*. 2020;*5*(6):460–75.
146. Sun C, Liu L-M, Selloni A, Lu GQ, Smith SC. Titania-water interactions: a review of theoretical studies. *J Mater Chem*. 2010;*20*(46):10319–34.
147. Selçuk S, Selloni A. Excess electrons at anatase TiO_2 surfaces and interfaces: insights from first principles simulations. *J Phys D: Appl Phys*. 2017;*50*(27):273002.
148. Bourikas K, Kordulis C, Lycourghiotis A. Titanium dioxide (anatase and rutile): surface chemistry, liquid–solid interface chemistry, and scientific synthesis of supported catalysts. *Chem Rev*. 2014;*114*(19):9754–823.
149. Hosseinpour S, Tang F, Wang F, Livingstone RA, Schlegel SJ, Ohto T, et al. Chemisorbed and physisorbed water at the TiO_2/water interface. *J Phys Chem Lett*. 2017;*8*(10):2195–9.
150. Calegari Andrade MF, Ko H-Y, Car R, Selloni A. Structure, polarization, and sum frequency generation spectrum of interfacial water on anatase TiO_2. *J Phys Chem Lett*. 2018;*9*(23):6716–21.
151. Futera Z, English NJ. Exploring rutile (110) and Anatase (101) TiO_2 water interfaces by reactive force-field simulations. *J Phys Chem C*. 2017;*121*(12):6701–11.
152. Holmström E, Ghan S, Asakawa H, Fujita Y, Fukuma T, Kamimura S, et al. Hydration structure of Brookite TiO_2(210). *J Phys Chem C*. 2017;*121*(38):20790–801.
153. Zheng Z, Huang B, Lu J, Wang Z, Qin X, Zhang X, et al. Hydrogenated titania: synergy of surface modification and morphology improvement for enhanced photocatalytic activity. *Chem Commun*. 2012;*48*(46):5733–5.
154. Tan T, Xie J, Wang W, Ping H, Ma P, Xie H, et al. A bio-inspired strategy for enhanced hydrogen evolution: carbonate ions as hole vehicles to promote carrier separation. *Nanoscale*. 2019;*11*(24):11451–6.
155. Fujishima A, Honda K. Electrochemical photolysis of water at a semiconductor electrode. *Nature*. 1972;*238*(5358):37–8.
156. Li Y-F, Liu Z-P, Liu L, Gao W. Mechanism and activity of photocatalytic oxygen evolution on titania anatase in aqueous surroundings. *J Am Chem Soc*. 2010;*132*(37):13008–15.
157. Valdés Á, Qu ZW, Kroes GJ, Rossmeisl J, Nørskov JK. Oxidation and photo-oxidation of water on TiO_2 surface. *J Phys Chem C*. 2008;*112*(26):9872–9.
158. Li Y-F, Selloni A. Pathway of photocatalytic oxygen evolution on aqueous TiO_2 anatase and insights into the different activities of anatase and rutile. *ACS Catal*. 2016;*6*(7):4769–74.
159. Imanishi A, Okamura T, Ohashi N, Nakamura R, Nakato Y. Mechanism of water photooxidation reaction at atomically flat TiO_2 (rutile) (110) and (100) surfaces: dependence on solution pH. *J Am Chem Soc*. 2007;*129*(37):11569–78.

160. Nakamura R, Okamura T, Ohashi N, Imanishi A, Nakato Y. Molecular mechanisms of photoinduced oxygen evolution, Pl emission, and surface roughening at atomically smooth (110) and (100) n-TiO_2 (rutile) surfaces in aqueous acidic solutions. *J Am Chem Soc*. 2005;*127*(37):12975–83.
161. Nakamura R, Nakato Y. Primary intermediates of oxygen photoevolution reaction on TiO_2 (rutile) particles, revealed by in situ FTIR absorption and photoluminescence measurements. *J Am Chem Soc*. 2004;*126*(4):1290–8.
162. Stecher T, Reuter K, Oberhofer H. First-principles free-energy barriers for photoelectrochemical surface reactions: proton abstraction at TiO_2 (110). *Phys Rev Lett*. 2016;*117*(27):276001.
163. Wang H-L, Hu Z-P, Li H. Dissociation of liquid water on defective rutile TiO_2 (110) surfaces using ab initio molecular dynamics simulations. *Front Phys*. 2018;*13*(3):138107.
164. Selcuk S, Selloni A. Facet-dependent trapping and dynamics of excess electrons at anatase TiO_2 surfaces and aqueous interfaces. *Nat Mater*. 2016;*15*:1107–12.
165. Mücksch C, Urbassek HM. Accelerated molecular dynamics study of the effects of surface hydrophilicity on protein adsorption. *Langmuir*. 2016;*32*(36):9156–62.
166. YazdanYar A, Aschauer U, Bowen P. Adsorption free energy of single amino acids at the rutile (110)/water interface studied by well-tempered metadynamics. *J Phys Chem C*. 2018;*122*(21):11355–63.
167. Zheng T, Wu C, Chen M, Zhang Y, Cummings PT. Molecular mechanics of the cooperative adsorption of a pro-Hyp-Gly tripeptide on a hydroxylated rutile TiO_2(110) surface mediated by calcium ions. *Phys Chem Chem Phys*. 2016;*18*(29):19757–64.
168. Wang M, Wang Q, Wang K, Lu X. Functionalized TiO_2 surfaces facilitate selective receptor-recognition and modulate biological function of bone morphogenetic Protein-2. *J Phys Chem C*. 2018;*122*(51):29319–29.
169. Mysen B, Richet P. CHAPTER 9 - Structure of aluminosilicate glass and melt. *Silicate glasses and melts*. 2nd ed. Amsterdam, Netherlands: Elsevier; 2019. p. 301–48.
170. Quezada GR, Rozas RE, Toledo PG. Ab initio calculations of partial charges at kaolinite edge sites and molecular dynamics simulations of cation adsorption in saline solutions at and above the pH of zero charge. *J Phys Chem C*. 2019;*123*(37):22971–80.
171. Chen Z, Zhao Y, Xu X, Liu C, Yang L. Structure and dynamics of Cs^+ in kaolinite: insights from molecular dynamics simulations. *Comput Mater Sci*. 2020;*171*:109256.
172. Zeitler TR, Greathouse JA, Cygan RT, Fredrich JT, Jerauld GR. Molecular dynamics simulation of resin adsorption at kaolinite edge sites: effect of surface deprotonation on interfacial structure. *J Phys Chem C*. 2017;*121*(41):22787–96.
173. Kobayashi K, Liang Y, Amano K-I, Murata S, Matsuoka T, Takahashi S, et al. Molecular dynamics simulation of atomic force microscopy at the water–muscovite interface: hydration layer structure and force analysis. *Langmuir*. 2016;*32*(15):3608–16.
174. Kobayashi K, Liang Y, Murata S, Matsuoka T, Takahashi S, Nishi N, et al. Ion distribution and hydration structure in the stern layer on muscovite surface. *Langmuir*. 2017;*33*(15):3892–9.
175. Jia Z, Li X, Zhu C, Yang S, Yang G. Reversal of cation-specific effects at the interface of mica and aqueous solutions. *J Phys Chem C*. 2018;*122*(10):5358–65.
176. Vogiatzis KD, Polynski MV, Kirkland JK, Townsend J, Hashemi A, Liu C, et al. Computational approach to molecular catalysis by 3d transition metals: challenges and opportunities. *Chem Rev*. 2019;*119*(4):2453–523.
177. Szabová L, Tateyama Y, Matolín V, Fabris S. Water adsorption and dissociation at metal-supported ceria thin films: thickness and Interface-proximity effects studied with DFT+U calculations. *J Phys Chem C*. 2015;*119*(5):2537–44.
178. Farnesi Camellone M, Negreiros Ribeiro F, Szabová L, Tateyama Y, Fabris S. Catalytic proton dynamics at the water/solid interface of ceria-supported Pt clusters. *J Am Chem Soc*. 2016;*138*(36):11560–7.
179. Szabová L, Camellone MF, Ribeiro FN, Matolín V, Tateyama Y, Fabris S. Dynamical solvent effects on the charge and reactivity of ceria-supported Pt nanoclusters. *J Phys Chem C*. 2018;*122*(48):27507–15.
180. Muñoz-Santiburcio D, Farnesi Camellone M, Marx D. Solvation-induced changes in the mechanism of alcohol oxidation at gold/titania nanocatalysts in the aqueous phase versus gas phase. *Angew Chem Int Ed*. 2018;*57*(13):3327–31.
181. Cai Q, Lopez-Ruiz JA, Cooper AR, Wang J-G, Albrecht KO, Mei D. Aqueous-phase acetic acid ketonization over monoclinic zirconia. *ACS Catal*. 2017;*8*(1):488–502.
182. Kitadai N, Oonishi H, Umemoto K, Usui T, Fukushi K, Nakashima S. Glycine polymerization on oxide minerals. *Orig Life Evol Biosph*. 2017;*47*(2):123–43.
183. Erastova V, Degiacomi MT, Fraser D, Greenwell HC. Mineral surface chemistry control for origin of prebiotic peptides. *Nat Commun*. 2017;*8*(1):2033.
184. Wang H, Ma C, Zhou L. A brief review of machine learning and its application. In 2009 International Conference on Information Engineering and Computer Science; 2009.
185. Behler J, Parrinello M. Generalized neural-network representation of high-dimensional potential-energy surfaces. *Phys Rev Lett*. 2007;*98*(14):146401.
186. Behler J. Constructing high-dimensional neural network potentials: a tutorial review. *Int J Quantum Chem*. 2015;*115*(16):1032–50.
187. Han Jiequn, Zhang Linfeng, Car Roberto, E Weinan. Deep Potential: A General Representation of a Many-Body Potential Energy Surface. *Communications in Computational Physics*. 2018;*23*(3).
188. Zhang L, Han J, Wang H, Car R, E W. Deep potential molecular dynamics: a scalable model with the accuracy of quantum mechanics. *Phys Rev Lett* 2018;*120*(14):143001.

189. Lu D, Wang H, Chen M, Liu L, Lin L, Car R, et al. 86 PFLOPS deep potential molecular dynamics simulation of 100 million atoms with ab initio accuracy. *Comput Phys Commun*. 2021;*259*:107624.
190. Gartner TE, Zhang L, Piaggi PM, Car R, Panagiotopoulos AZ, Debenedetti PG. Signatures of a liquid–liquid transition in an ab initio deep neural network model for water. *Proc Natl Acad Sci U S A*. 2020;*117*(42):26040–6.
191. Quaranta V, Hellström M, Behler J. Proton-transfer mechanisms at the water–ZnO interface: the role of presolvation. *J Phys Chem Lett*. 2017;*8*(7):1476–83.
192. Calegari Andrade MF, Ko H-Y, Zhang L, Car R, Selloni Annabella. Free energy of proton transfer at the water–TiO_2 interface from ab initio deep potential molecular dynamics. *Chemical Science*. 2020;*11*(9):2335–41.
193. Hellström M, Quaranta V, Behler J. One-dimensional vs. two-dimensional proton transport processes at solid–liquid zinc-oxide–water interfaces. *Chem Sci*. 2019;*10*(4):1232–43.
194. Quaranta V, Behler J, Hellström M. Structure and dynamics of the liquid–water/zinc-oxide interface from machine learning potential simulations. *J Phys Chem C*. 2019;*123*(2):1293–304.
195. Singraber A, Behler J, Dellago C. Library-based LAMMPS implementation of high-dimensional neural network potentials. *J Chem Theory Comput*. 2019;*15*(3):1827–40.
196. Qi Y, Lee J, Klauda JB, Im W. CHARMM-GUI Nanodisc builder for modeling and simulation of various nanodisc systems. *J Comput Chem*. 2019;*40*(7):893–9.
197. O'Connor M, Deeks HM, Dawn E, Metatla O, Roudaut A, Sutton M, et al. Sampling molecular conformations and dynamics in a multi-user virtual reality framework. *Sci Adv*. 2018;*4*(6):eaat2731.
198. Verma PK, Kundu A, Puretz MS, Dhoonmoon C, Chegwidden OS, Londergan CH, Cho M. The bend+libration combination band is an intrinsic, collective, and strongly solute-dependent reporter on the hydrogen bonding network of liquid water. *J Phys Chem B*. 2018;*122*(9):2587–99.
199. Isaienko O, Nihonyanagi S, Sil D, Borguet E. Observation of the bending mode of interfacial water at silica surfaces by near-infrared vibrational sum-frequency generation spectroscopy of the [stretch + bend] combination bands. *J Phys Chem Lett*. 2013;*4*(3):531–5.

How to cite this article: Wang R, Klein ML, Carnevale V, Borguet E. Investigations of water/oxide interfaces by molecular dynamics simulations. *WIREs Comput Mol Sci*. 2021;e1537. https://doi.org/10.1002/wcms.1537